The
ENGINEERS' DIGEST

REVIEW OF ENGINEERING PROGRESS ABROAD

ENGINEERING LIBRARY
MAR 2 1949

VOL. X. No. 2 FEBRUARY, 1949

High Carbon ·004" to ·020" thick.
Our strip rolling plant has been laid down specially for producing bright cold rolled strip steel only in these thin sizes and high carbons. We do not manufacture soft strip of the deep-drawing quality.
COLD ROLLED BRIGHT STEEL STRIP
TOOL STEELS. BAND SAWS. COLD SAWS SEGMENTAL SAWS.
SANDERSONS
of Sheffield
SANDERSON BROS & NEWBOULD LTD.
ATTERCLIFFE WORKS. SHEFFIELD.
ALLOY STEELS. CIRCULAR CUTTERS. HACKSAWS. FILES.

SPOT WELDING ALUMINIUM ALLOYS!

PHILIPS E.1504/AL SPOT WELDER
A moderately priced dual purpose machine for welding light gauge aluminium and mild steel.
IMMEDIATE DELIVERY FROM STOCK!

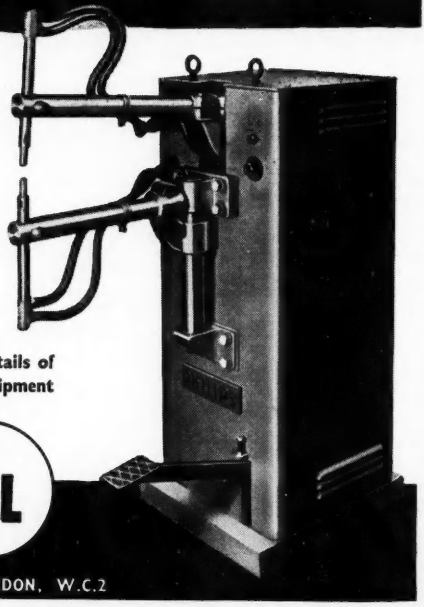

Write today for full details of the Philips 1504/AL equipment

RESISTANCE WELDING EQUIPMENT FROM
PHILIPS ELECTRICAL
LIMITED

INDUSTRIAL DEPT., CENTURY HOUSE, SHAFTESBURY AVENUE, LONDON, W.C.2

THE ENGINEERS' DIGEST

Published Monthly by Engineers' Digest Ltd., 120 Wigmore Street, London, W.1. Tel.: WELBECK 9357

VOL. X. No. 2. **Annual Subscription £2 2s. Single Copies 4s. 6d.** FEBRUARY, 1949

IN THIS ISSUE

THE article overleaf on the calculation of rockets develops equations for estimating the velocity at the end of combustion, the maximum altitude, and the range of low-flying and stratospheric rockets. It also determines the mechanical and overall efficiencies of rockets in the ideal case where there is no air resistance or retardation due to gravity, and in cases where air resistance and gravity effects exist, taking into account the relative mass-ratio of the propellent and rocket body to the warhead constituting the useful load, and indicating the conditions under which optimum propulsive efficiency can be obtained.

* * *

A new welding process was introduced at the National Metal Show in Philadelphia in October, 1948. This process, known as the " Aircomatic " process, may be used for welding heavy sections of aluminium and aluminium alloys at wire feed speeds ranging from 100 to 300 inches per minute, permitting deposition rates in excess of those attained by the usual welding methods. The process, which is described in detail on page 59, combines the desirable features of both metal arc welding and inert gas-shielded arc welding, and should be of considerable interest both to producers and fabricators of aluminium alloys.

* * *

The basis for rational climb requirements is investigated in the article on page 42. It is suggested that climb requirements should fall into three sections, viz. (a) a flat minimum value for rate of climb ; (b) a lower limiting value for rate of climb, directly proportional to the stalling speed, or a flat minimum value for the gradient of flight path (dependent on the flight conditions considered) ; (c) if necessary, an upper limiting value for rate of climb directly proportional to the stalling speed.

Sections (b) and (c) are shown to cover rational requirements for manoeuvrability. In this respect, the basic idea is that all aeroplanes requiring approximately equal take-off distances should have approximately equal manoeuvrability characteristics. The minimum radius of turn in horizontal flight is considered as a measure of the manoeuvrability, while, according to other publications, a criterion for the required take-off distance is formed approximately by the product of wingloading and powerloading.

The considerations given are based on simplified relations, so that they cannot give a sufficient basis for specifying numerical values. Some quantitative examples, however, are presented to show the trend in these values and to give guidance in drawing up ultimate standards.

* * *

A calculation of the effective moment of inertia of shafts with a transverse hole is given on page 51, and the nominal and effective maximum stresses in the neighbourhood of the hole are determined by means of form factors for static and dynamic, torsional and combined torsion-and-bending loads. The investigation includes, furthermore, a series of tests on various specimens with transverse holes of increasing diameter, and the numerical values for the form factors thus obtained will enable designers to determine effective peak stresses for shafts with oil holes or other passages perpendicular to the shaft axis. The report also deals with the fatigue strength and the yield point of torsionally stressed specimens.

* * *

Stepless regulation of speed achieved by purely mechanical transmission is well known in this country and was applied to motor cars of certain makes before the war. It is believed, however, that the application to tractors is a novel feature, and the abstract on page 53 dealing with this matter clearly demonstrates the advantages of gearless drive, if it will stand the test of the severe conditions under which tractors for agricultural purposes are normally used.

* * *

The widespread use of controlled-atmosphere furnaces is in large measure due to progressive study and understanding of the effect of atmosphere gases on the carbon content of steel during heat treatment. A direct result of this study and work has been the accumulation of valuable data on the equilibrium conditions for various atmosphere compositions and carbon contents. Because of this knowledge, gas atmospheres are used with marked success in carburizing, carbo-nitriding, carbon restoration, malleablizing, normalizing, bright annealing and other heat-treatment processes. The article on page 57 outlines the basic facts of gaseous equilibrium and describes the use of equilibrium curves in the control of carbon concentration.

Calculation of Rockets

By G. AZZONI. (From *Rivista Marittima*, Technical Supplement, July, 1948, pp. 169-196, 8 illustrations.)

THE rocket is a projectile which is accelerated by the forward thrust of gases flowing out of the projectile itself until a certain terminal velocity is attained, after which the remainder of the trajectory is completed without any further thrust being developed.

1. IDEAL CASE

Assuming that air resistance and the retarding component due to gravity are equal to zero, the equation of motion is

$$\frac{P}{g}\,dw = -\,U\,\frac{dP}{g}, \text{ or}$$

$$dw = -\,U\,dP/P \qquad \ldots \qquad (1)$$

where w = velocity of projectile, P = mass of projectile at a given instant, U = exhaust velocity of gases after combustion. Denoting by R the weight of the rocket empty and by C the weight of the propellent charge, and using the ratios $x = C/R$, and $q = C/(C + R)$, and taking W as the rocket velocity at the end of combustion, we have

$$\int_0^W dw = -\,U \int_{R+C}^{R} dP/P$$

assuming U is constant, which is equivalent to assuming that the gas temperature is practically constant throughout combustion. The integration gives

$$W = U \ln [(R + C)/R] \text{ or}$$

$$W/U = \ln [(R + C)/R] = \ln (1 + x) = \ln [1/(1 - q)] \quad (2)$$

where ln = log to the base e. The values of W/U plotted against x are given in Fig. 1, whereas W/U as a function of q is shown in Fig. 2.

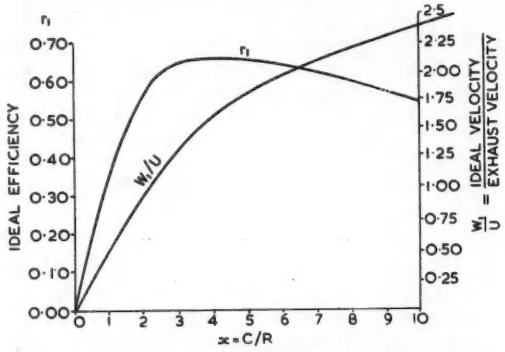

Fig. 1. **Theoretical efficiency r_1 and theoretical velocity ratio W_1/U as functions of $x = C/R$.**

The overall propulsive efficiency η is equal to the ratio of the kinetic energy of the rocket at the end of the combustion of the propellent charge, to the mechanical equivalent of the thermal energy liberated by the combustion of the charge:

$$\eta = \frac{RW^2}{2g}\,\frac{1}{EQC} = \frac{U^2}{2gEQ}\,\frac{RW^2}{CU^2} \qquad \ldots \qquad (3)$$

where E = 427 kg m/cal = mechanical equivalent of heat, Q = calorific energy of the propellant (cal/kg). The exhaust velocity is $U = \sqrt{2gE\Delta Q}$, where ΔQ = quantity of thermal energy converted into kinetic energy of the gas. Therefore, $\Delta Q/Q = U^2/(2gEQ)$ is the thermodynamic efficiency η_t of the exhaust, assuming zero friction and no vortices. If r_1 = mechanical efficiency in the ideal case, then the overall propulsive efficiency will be $\eta = \eta_t\, r_1 = \eta_t\, RW^2/(CU^2)$, and we have

$$r_1 = RW^2/(CU^2) = \frac{R}{C}\,[\ln (1 + x)]^2$$

$$= \frac{1}{x}\,[\ln (1+x)]^2 = \frac{1-q}{q}\left[\ln \frac{1}{1-q}\right]^2 \qquad (4)$$

The values of $r_1 = r_1\,(x)$ and $r_1 = r_1\,(q)$ are given in Figs. 1 and 2.

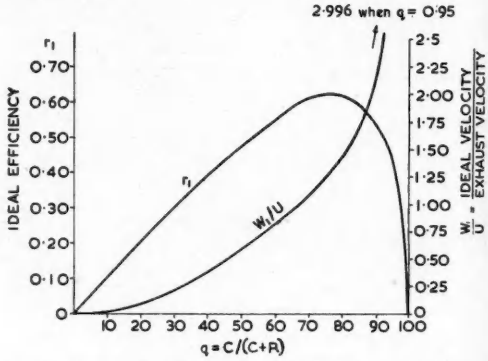

Fig. 2. **Theoretical efficiency r_1 and velocity ratio W_1/U as functions of $q = C/(C + R)$.**

Differentiating the expression for r_1 and equating to zero, we find a single maximum of $r_1 = 0{\cdot}648$ when $\ln (1 + x) = 2x/(1 + x)$, that is, when the weight of the charge is slightly more than 4 times the weight of the rocket empty (or approximately 80 per cent of the total weight with full load). This result is illustrated in Figs. 1 and 2, which also enable determination of (a) the terminal velocity W that can be obtained with a given value of the charge C, and (b) the weight of the charge C required to obtain a given value of W, when the exhaust velocity U of the gases and the empty weight R of the rocket are known.

2. LOW-FLYING ROCKETS WITH HIGH ACCELERATION

If air resistance and the retarding component of gravity are taken into account, the equation of motion becomes

$$-\,U\,\frac{dP}{g} = \frac{P}{g}\,dw + \frac{P}{g}\,\rho\,dt + \frac{10^3\,\delta\,i\,a^2}{g}\,F(W)\,dt \qquad \ldots \qquad (5)$$

where $\rho = g \sin \varphi$ = component of gravity retarding motion. Dividing by P/g and integrating, we obtain

$$U \ln [(R + C)/R] = W + \rho\,T + \int_0^T \frac{10^3\,i\,\delta\,a^2\,F(W)}{P}\,dt \quad (6)$$

where δ = ballistic density of the air, i = form factor,

$F(W)$ = resistance function (Siacci), a = outside diameter of the rocket, and T = duration of combustion.

Assuming for an approximation that $\delta = \delta_0 = 1$, that P can also be obtained from the expression $w = U \ln [(R + C)/P]$, and that the mean value of the retardation due to air resistance is equal to that at the instant for which $w = W/2$, we have

$$\ln [(R + C)/P_m] = W/(2U) = \frac{1}{2} \ln [(R + C)/R] \quad (7)$$

hence

$$\ln P_m = \frac{1}{2} [\ln (R + C) + \ln R], \text{ and}$$

$$P_m = \sqrt{R^2 + RC} = R\sqrt{1 + x}.$$

Therefore

$$U \ln [(R + C)/R] = W_1$$

$$= W_2 + \rho T + \frac{10^3 i \delta_0 a^2}{R\sqrt{1 + x}} F(W_2/2)T \quad .. \quad (8)$$

W_2 is the effective velocity of the rocket at the end of the combustion of the charge. The above expression can be rewritten as

$$W_1 = W_2 + \rho T + \frac{T F (W_2/2)}{C' \sqrt{1 + x}} \quad .. \quad (9)$$

where C′ is the reduced ballistic coefficient of the rocket at the end of combustion: $C' = R/(10^3 \delta_0 i a^2)$.

Indroducing the mean value $\sigma' = dw/dt$ (mean) $= W_2/T$, we have

$$W_1 = W_2 \left[1 + \frac{\rho}{\sigma'} + \frac{F (W_2/2)}{C' \sigma' \sqrt{1 + x}} \right]$$

$$= W_2 (1 + \epsilon + \zeta) \quad .. \quad .. \quad .. \quad (10)$$

where $\epsilon = \rho/\sigma'$, and $\zeta = F (W_2/2)/[C' \sigma' \sqrt{1 + x}]$.

If we do not regard as useful work the increase in potential energy of the rocket due to its ascent, the effective mechanical efficiency r_2 will be proportional to the square of the velocity attained, and, therefore, the ratio of r_2 to the theoretical mechanical efficiency r_1 will be equal to W_2^2/W_1^2, so that

$$r_2 = \frac{r_1}{[1 + \epsilon + \zeta]^2} \quad .. \quad .. \quad (11)$$

and neglecting the terms with $1/\sigma'^2$ in view of the large value assumed for σ' we have

$$r_2 = \frac{r_1}{1 + 2\epsilon + 2\zeta} \quad .. \quad .. \quad (12)$$

If we regard the increase in altitude y also as useful work, the efficiency r_2 will be proportional to $W_2^2 + 2gY$; therefore,

$$W_2^2 + 2gY = W_2^2 + 2g \frac{\sigma'}{2} T^2 \sin^2 \varphi$$

$$= W_2^2 (1 + \epsilon) \quad .. \quad .. \quad (13)$$

(apart from the constant $R/(2g)$), where Y is the altitude reached at the end of combustion. Therefore,

$$r_2' = r_2 (1 + \epsilon) = \frac{r_1 (1 + \epsilon)}{1 + 2\epsilon + 2\zeta}$$

$$= \frac{r_1}{\frac{1 + \epsilon}{1 + \epsilon} + \frac{\epsilon + 2\zeta}{1 + \epsilon}} = \frac{r_1}{1 + \frac{\epsilon + 2\zeta}{1 + \epsilon}} \quad .. \quad (14)$$

Thus, if ϵ is neglected in the expression $1 + \epsilon$, since it is assumed that $\rho/\sigma' \ll 1$, we have for the effective mechanical efficiency, including the work due to the increase in potential energy,

$$r_2' = r_1 \frac{1}{1 + \epsilon + 2\zeta} \quad .. \quad .. \quad (15)$$

It is, therefore, possible to obtain approximate values for the effective velocity W_2, and the effective efficiencies r_2 and r_2', from the theoretical values, by means of the three relations

$$\left.\begin{aligned} W_2 &= W_1/(1 + \epsilon + \zeta) \\ r_2 &= r_1/(1 + 2\epsilon + 2\zeta) \\ r_2' &= r_1/(1 + \epsilon + 2\zeta). \end{aligned}\right\} \quad .. \quad (16)$$

Therefore, either the terminal velocity W_2 can be determined, when C, the weight of the propellent charge, is known, or conversely, C can be obtained if W_2 is given. In general, it will be necessary to determine W_2 by successive approximations.

The value of σ' or x can be obtained from $\sigma' = W_2/T = W_2 A/V_0$, where A = propellent coefficient, P = pressure in the combustion chamber (constant pressure if U is assumed to be constant), and $V_0 = \int_0^1 dz/\varphi(z)$, where $\varphi(z)$ is a form function of the propellent. The above formulae show that the efficiency increases with the mean value of the acceleration σ'.

An increase in the weight of the propellent charge generally involves an increase in the size of both the combustion chamber and the exhaust nozzle, that is, an increase in the rate of mass flow per unit time. Since $\sigma' = dw/dt \cong UdP/(Pdt)$, the value of σ' varies roughly as the mass flow per second; we can, therefore, conclude that when x is increased, $F(W/2)$ also increases, but this is compensated by a similar increase in the denominator of the product $\sigma' \sqrt{1 + x}$. As a result of this approximation, it can be said that W_2, r_2, r_2' always remain smaller than W_2 and r_1, but follow their variations as functions of x.

3. STRATOSPHERIC ROCKETS WITH LOW ACCELERATION AND NEARLY VERTICAL TRAJECTORY DURING COMBUSTION

The equation of motion is

$$-U \frac{dP}{g} = \frac{P}{g} dw + \frac{P}{g} g\, dt + \frac{10^3 \delta i a^2}{g} F(W)\, dt \quad (17)$$

where δ, however, is no longer constant, but varies with altitude according to Laplace's empirical approximation $\delta_y = \delta_0 \exp(-8sy) = \delta_0 \exp(-hy)$, where $s = h/8$ and $h = 10^{-4}$.

Assuming as a mean value for the retardation the value obtained for $t = T/2$, and regarding the motion as being uniformly accelerated motion, so that σ = constant $= dw/dt$ (mean) $= \sigma'$, we have

$$w_m = W/2;\ y_m = Y/4 = \sigma T^2/8;\ P_m = R\sqrt{1 + x}$$

$$U \ln [(R + C)/R] = W_1 = W_3 + gT + T e^{-2sY} \lambda \quad (18)$$

$$= W_3 [1 + \frac{g}{\sigma} + \lambda e^{-2sY}],$$

where $\lambda = F(W_3/2)/[C' \sigma \sqrt{1 + x}]$

Substituting $F(W) = W^2 K(W)$, we have

$$W_1 = W_3 \left[1 + \frac{g}{\sigma} + \frac{W_3^2}{2\sigma} \mu \right] \quad .. \quad (19)$$

where $\mu = e^{-2sY} K(W_3/2)/[2C' \sqrt{1 + x}]$

As σ is assumed to be constant, so that $Y = \sigma T^2/2 = W_3^2/(2\sigma)$, the following can be written:—

$$W_3 = W_1 \Big/ \left[1 + \frac{2gY}{W_3^2} + \mu Y \right] = W_1/H_3$$

$$r_3' = r_3 \left(1 + \frac{2gY}{W_3^2} \right) = r_3 H_3' \quad .. \quad .. \quad (20)$$

$$r_3 = r_1 \Big/ \left[1 + \frac{2gY}{W_3^2} + \mu Y \right]^2 = r_1/H_3^2.$$

In these equations it is assumed that the altitude Y, at which combustion is completed, is known. If, instead, the mean value of acceleration σ is given, these equations become

$$W_3 = W_1 \Big/ \left[1 + \frac{g}{\sigma} + \lambda e^{-sW_3^2/\sigma} \right]$$

$$r_3' = r_3 \left(1 + \frac{g}{\sigma} \right) \quad .. \quad .. \quad .. \quad (21)$$

$$r_3 = r_1 \Big/ \left[1 + \frac{g}{\sigma} + \lambda e^{-sW_3^2/\sigma} \right]^2$$

It will be noticed that, for a given value of Y at the end of combustion, the expression in brackets decreases with increasing charge, since this determines an increase in W_3. In fact, $K(W_3/2)$ decreases as $W_3/2$ increases, when $W_3 > 1{,}040$ m/sec, a velocity which is nowadays considerably exceeded by rockets of this type. Therefore, when x increases, the numerator of the third term decreases and the denominator increases.

Thus, the variation of the quantities W_3, r_3, and r_3' follows that of W_1 and r_1, but with the maximum values displaced towards the right, and there is a longer section of the trajectory over which r can be regarded as constant when x is increased.

The curves of Figs. 1 and 2 can thus also be used for stratospheric rockets, provided the polynomials in brackets in equations (20) and (21) are calculated separately. As the unknowns W_3 or x are included in these expressions, successive approximations will have to be used.

4. EFFECT OF DEAD WEIGHTS

The previous treatment took into consideration the ratio C/R of the weight of the charge to the weight of the empty rocket, without making any restrictions as to its maximum value. However, in practice, an increase of the charge also involves a corresponding increase in the weight of the power plant components: propellant tank, combustion chamber, exhaust nozzle, etc.

In rockets, the only useful weight is that of the warhead, since although the increased weight of the empennage and similar components somewhat increases the penetrating power through the air after the end of the accelerated portion of the trajectory has been reached, this advantage is counterbalanced by the increased drag due to the larger size of the projectile. A further analysis will, therefore, be based on the useful weight, instead of on the empty weight as in the previous calculations.

It will be assumed for simplicity that the weight of accessory equipment, propellant tanks, combustion chamber, exhaust nozzle, etc., is proportional to the propellant charge, so that $R - Z = f\,C$, where Z = weight of warhead, and f = proportionality factor. It would be more accurate to put $R - Z = b + f\,C^{2/3}$, but this would complicate the calculation without affecting the general conclusions which can be derived. We now introduce the new ratio $z = (C + fC)/Z$ = ratio of the weight of the propellent charge plus accessories to the useful weight (warhead). The relation between x and z is

$$x = C/R = (C + fC)/(Z + fC) - fC/(Z + fC)$$

$$= \frac{1}{\dfrac{1}{z} + \dfrac{f}{1+f}} - \frac{fC}{\dfrac{fC + C}{z} + fC}$$

hence $$x = z/(1 + f + fz) \quad .. \quad .. \quad .. \quad (22)$$

The theoretical velocity is, therefore, given by

$$W_1 = U \ln [1 + \{ z/(1 + f + fz) \}].$$

Fig. 3 gives the values of W_1/U as functions of z, or the ratio of the propelling portion to the useful weight, for various values of f. The effective velocities W_2 and W_3 are again determined by eqs. (16) and (20).

The useful work done is represented by the kinetic (and possibly the potential) energy imparted to the warhead. Consequently, the mechanical efficiency of

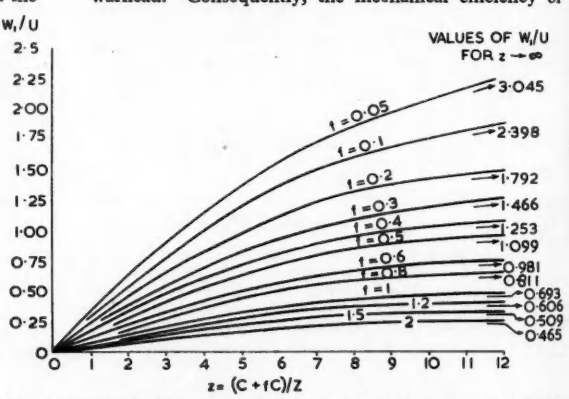

Fig. 3. **Theoretical velocity ratio W_1/U as a function of $z = (C + fC)/Z$ (ratio of propellent charge plus accessories to weight of warhead), for various values of the parameter f.**

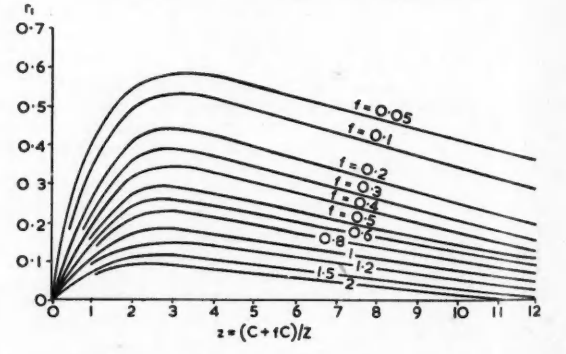

Fig. 4. **Variation of $\bar{r}_1$ (theoretical efficiency in which only the kinetic energy of the warhead is regarded as useful work) plotted against $z = (C + fC)/Z$ for various values of f (ratio of weight of accessories to weight of propellent charge).**

the propulsion can now be defined as

$$\bar{r} = ZW^2/(CU^2) = rZ/(Z + fC) \quad .. \quad .. \quad (23)$$

and, therefore,

$$\bar{r}_1 = r_1 Z/(Z + fC)$$

r_1 being determined by eq. (4) with x replaced by its value from eq. (22), hence

$$\bar{r}_1 = \frac{1+f}{z}\left[\ln\left(1 + \frac{z}{1+f+fz}\right)\right]^2 \quad .. \quad (24)$$

Fig. 4 gives the variation of $\bar{r}_1$ as a function of z for various values of the parameter f. The effective efficiencies can be obtained by means of the equations

$$\left.\begin{aligned} \bar{r}_2 &= \bar{r}_1/(1 + 2\epsilon + 2\zeta) \\ \bar{r}_3 &= \bar{r}_1/H_3^2 \\ \bar{r}_2' &= \bar{r}_1/(1 + \epsilon + 2\zeta) \\ \bar{r}_3' &= \bar{r}_3 H_3' \end{aligned}\right\} \quad .. \quad .. \quad .. \quad (25)$$

using eqs. (11) and (20).

5. CONCLUSIONS

1. The efficiency or degree of utilization of the propellent charge increases when the mean acceleration imparted to the rocket is increased, both in the case of low-flying and stratospheric projectiles. For the latter, however, the altitude Y reached at the end of combustion is the main factor, and not the mean acceleration.

In the correction polynomial H_3, the second term, $2gY/W_3^2$, increases linearly with Y, whereas the third term follows the course of Y exp $(-2sY)$, which is shown in Fig. 6. By equating the derivatives of this product to zero, it is found that Y exp $(-2sY)$ has a single maximum at $Y = 40$ km, and a single point of inflection at $Y = 80$ km. At this latter point the tangent to the function has a slope of only $-7° 45'$ relatively to the Y-axis. The linear increase of the second term compensates for any slight decreases of the third term, and, therefore, H_3 increases with Y.

The variation of H_3 (Y) is given in Fig. 7 for the numerical values $C' = 4$, $R = 4$ tons, $a = 1{\cdot}6$ metres, $i = 0{\cdot}4$, $W_3 = 1{,}600$ m/sec, $x = 2{\cdot}25$, $Z = 9$, and $f = 0{\cdot}3$. The curves of Figs. 6 and 7 are only approximations based on the simplifying assumptions regarding density, mean air resistance equal to air resistance at $t = T/2$, constant acceleration, etc. The effect of the correction polynomial H_3 can be appreciated from the following consideration: When $Y = 50$ km, we have $W_3/W_1 = 1/1{\cdot}677$, so that in order to obtain $W_3 = 1{,}600$ m/sec, it will be necessary to provide a charge capable of giving a theoretical velocity W_1 of about 2,700 m/sec. The mechanical efficiencies, instead of $r_1 = 62$ per cent, are $r_3 = 22$ per cent, $r_3' = 30$ per cent, and $r_3' = 10$ per cent.

From this investigation, it can be concluded that (1) for low-flying rockets the acceleration should be as high as possible; (2) for long-range stratospheric rockets, after determining the altitude beyond which the projectile does not encounter any appreciable air resistance, the projectile should be given a mean acceleration such that the required velocity will be attained without appreciably exceeding the maximum altitude determined.

2. Consideration of Fig. 1 shows that $x = C/R$ has a considerable effect on the velocity attained by the rocket, since within the range of x-values allowable in practice, a variation of x will simultaneously affect the quantity of energy required per unit weight of the empty rocket, and the mechanical efficiency.

Therefore, rockets using colloidal powders or similar fuels are extremely sensitive to working tolerances of both the weight of the empty projectile and of the charge, and, consequently, their firing is scattered and inaccurate. Beside this lack of accuracy, these projectiles have insufficient stability along their trajectory. It appears, however, that a gyroscopic stabilization of these rockets is being tried out by using multiple exhaust nozzles inclined at an angle relatively to the rocket axis.

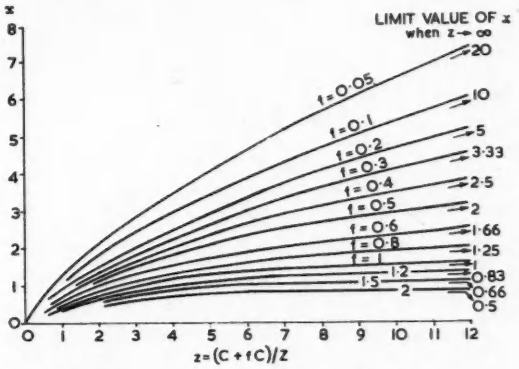

Fig. 5. **Variation of $x = C/R$ as a function of z, for various values of the parameter f.**

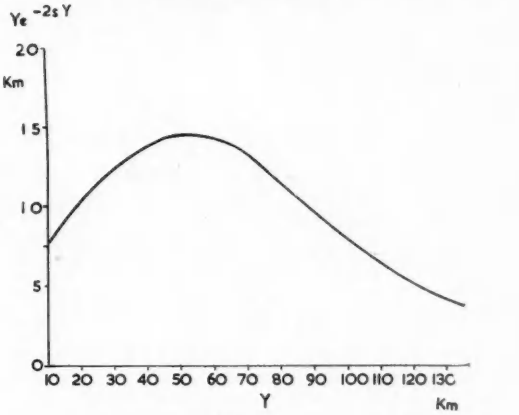

Fig. 6. **Variation of Ye^{-2sY} as a function of Y (the altitude at the end of combustion).**

Considering Figs. 2 and 6, it will be seen that the terminal velocity of the stratospheric rocket depends, to a great extent, on the correct adjustment of the fuel control system. This requirement can be satisfied by incorporating an automatic device which controls the fuel according to the velocity of the rocket, thus cancelling the inaccuracy in the altitude attained and the quantity of fuel consumed. The German V-2 had, for instance, an acceleration integrator which determined velocity by measuring $W = \int \sigma \, dt$.

3. It will be seen from Fig. 4 that for each value of f there is a maximum efficiency for a well-determined value of the ratio z of the weight of the propelling system to that of the warhead. When the value of f is between $0{\cdot}05$ and $2{\cdot}0$, the maximum efficiency is obtained approximately when $2{\cdot}7 \leq z \leq 1{\cdot}2$.

Fig. 3 shows, furthermore, that the increase in velocity is small when z is increased beyond the value corresponding to the maximum efficiency $\bar{r}_1$; it is,

therefore, unnecessary, in practice, to attain very high values of z. These figures also show that the velocity attainable with a rocket has a well-determined limit, as will be shown later. Even in the region where $\bar{r}_1$ has its maximum value, the overall efficiency is very low. In fact, the theoretical mechanical efficiency as given by Fig. 3 should be divided by the square of the correction polynomial, and then multiplied by the thermodynamic efficiency of the exhaust.

Taking the case of a V-2 type projectile, and assuming that the data published on this rocket are correct, in which case $C = 9$ tons of ethyl alcohol and oxygen, $R = 4$ tons, $Z = 1{\cdot}3$ tons, $W_3 = 1{,}600$ m/sec, $Y = 50$ km, we have

$$\bar{r}_1 = 0{\cdot}2,\ r_3 = \bar{r}_1/(1{\cdot}677)^2,\ \bar{r}_3' = 0{\cdot}071 \times 1{\cdot}35 = 0{\cdot}96.$$

If the thermodynamic efficiency is $\eta_t = 30$ per cent, as claimed, we finally obtain an overall efficiency $\eta = \bar{r}_3\,\eta_t = 2{\cdot}2$ per cent, and $\bar{\eta}' = \bar{r}'\,\eta_t = 3$ per cent.

If the efficiency calculation is made for a normal projectile with balistite, values of the same order of magnitude are obtained, since f is very high, while the correction polynomial has an almost negligible effect. Considering, for instance, a British rocket projectile of 82·5 mm, for which $Z = 11$ kg, $C = 5{\cdot}8$ kg of balistite with a low nitroglycerine content, and approximately 10 per cent centralite, so that for an overall value we can assume $Q = 1100$ cal/kg; $R\text{-}Z = 8{\cdot}2$ kg; then $f = 1{\cdot}45$ and $z = 1{\cdot}27$. Assuming again that $\eta_t = 30$ per cent, and $H_3 = 1$, we have $r_1 = 13$ per cent, $\eta = 0{\cdot}13 \times 0{\cdot}3 \simeq 4$ per cent.

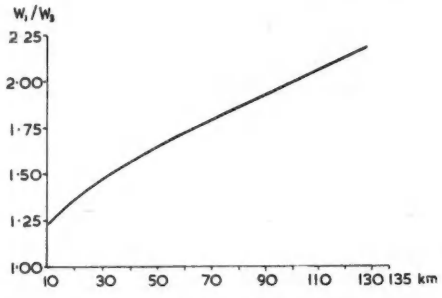

Fig. 7. **Variation of the correction polynomial $H_3 = W_1/W_3$ as a function of Y, assuming $C' = 4$, $x = 2{\cdot}25$, $W_3 = 1{,}600$ m/sec.**

These overall efficiencies are much lower than those obtained with cannon-type projectiles, which have a mean efficiency η of 30-40 per cent. It may be said that low-flying rockets will only be an advantage in the case of short distances (less than 5-6 km), where accuracy of fire is not the primary consideration. The cannon will remain unchallenged for ranges between 5-6 and 40-50 km. Beyond this distance, the stratospheric rocket will be used.

4. In regard to rockets, there are other factors besides z which can affect the value of the terminal velocity W. One of these is the exhaust velocity $U = \sqrt{2gE\Delta Q} = \sqrt{2gEQ\eta_t}$. If all the constant quantities are represented by a constant b, and the corresponding expression is substituted for η_t, we have

$$U = \sqrt{bP'v} \times \sqrt{1 - \frac{n-1}{n}\left(\frac{p''}{p'}\right)},$$

where v is the specific volume of the burnt gases, and p', p'' are the gas pressures at the initial and end cross-sections of the exhaust nozzle, respectively.

W_3 can be increased either by obtaining a higher thermodynamic efficiency, or by using a fuel with a higher calorific value. An increase of η_t depends on the ratio of p''/p', and, therefore, on the length of the exhaust nozzle, so that this would require a heavier nozzle, and hence cause an increase of f, which has a detrimental effect. Thus, W will not increase proportionately to U when this method is applied.

An increase of Q which is proportional to the product $p'v$, where p' and v are the pressure and the specific volume of the gases in the combustion chamber, will cause a rise in the value of U. If p' is increased, heavier walls will be required for the combustion chamber to resist the higher pressure, and, therefore, f will increase and reduce the gain obtained with U. However, if v is increased, U will be raised to a higher value without requiring thicker walls for higher pressures, although higher temperatures will be obtained. Furthermore, the correction polynomial, H_3, will not vary appreciably, so that the mean thrust will not be reduced. In fact, the mass flowing out per unit time is proportional to U/v and, therefore, thrust is proportional to U^2/v, and as $U \propto \sqrt{v}$, we see that thrust does not vary with variations of v, because p' is not changed.

In conclusion, it will be advantageous to have a fuel with a high calorific value burning at a slower rate, so that without increasing pressure, a thrust equal to that obtained with a poorer fuel is obtained over a longer period of time. The velocity of combustion will be proportional to $1/\sqrt{Q}$, while the duration of combustion is proportional to $\sqrt{Q}$; hence, with a constant thrust, $W \propto \sqrt{Q}$. Thus, the great advantage that the rocket has over the cannon is its possibility, at least in theory, of using a fuel with a greater calorific power. The maximum value of Q for an oxygen-hydrogen combustion for a stratospheric rocket is $Q = 3{,}200$ cal/kg., and this is approximately 1·5 times greater than the heat produced by ethyl alcohol and oxygen (2,080 cal/kg). Ethyl ether, benzol, methane, and acetylene can produce quantities of heat ranging between 2,200 and 2,800 cal/kg. (See: A.N.V. Ré: Stratospheric projectiles, "Rivista Aeronautica," March-April, 1946.) For low-flying rockets, which now use balistite more or less attenuated, it cannot be foreseen whether it will be possible to adapt these to use liquid fuels which would give the two-fold advantage of a higher Q and a lower f value. An increase of Q could be obtained by mixing the balistite with powders of aluminium, boron, beryllium, magnesium, silicon, etc., which develop approximately 3,000 cal/kg in combustion with oxygen, the problem of the higher temperatures developed in these reactions also requiring further consideration. Further improvement may be achieved by reducing the weight of auxiliary and controlling devices, fuel pumps, servo-motors, etc. Some long-range projectiles have been reported to have a value $x = 9$, equivalent to a value $f = 0{\cdot}05\text{-}0{\cdot}10$.

5. The negative influence of f can also be reduced by designing multi-stage rockets, so that the kinetic energy stored in the rocket body can be transferred to the warhead when this severs from the body. A long-range rocket of this type was the A-9, which consisted of a V-2 weighing 13 tons, mounted on an "impulsor" rocket of larger size weighing 80 tons; combustion of the V-2 charge was initiated when the charge of the impulsor was completely consumed, and the mass of the impulsor was then released giving a corresponding quantity of energy to the mass of the V-2 component. The formulae derived above cannot be applied to rockets with two or more stages because of the sudden jump of the exhaust velocity U at the instant when the mass decrease is almost exclusively due to the discharge of the main rocket body. If we simplify this problem by assuming that the accessory weights only behave as kinetic energy accumulators, we find that the terminal velocity of the warhead has roughly its previous value multiplied by $(Z + fC)/Z = (1 + f + fz)/(1 + f)$.

Residual Stresses in Rolled Sheet

By YA. S. GALLAI, M. I. ZLOTNIKOV and N. N. SOKOLOVSKI. (From *Stal*, No. 1, 1948, pp. 37-45, 14 illustrations.)

IN the rolling of thin steel sheet, residual stresses remain in the metal which are due to uneven deformation over the width of the sheet. The materials investigated were the following:—

No. (1) 0·32-0·42 per cent carbon.
0·4-0·7 per cent manganese.
0·15-0·35 per cent silicon.
0·8-1·2 per cent chromium.
0·2 per cent nickel.

No. (2) 0·16 per cent carbon.
0·8-1·1 per cent manganese.
0·6-0·9 per cent silicon.

No. (3) 0·65-0·75 per cent carbon.
0·45-0·8 per cent manganese.
0·15-0·4 per cent silicon.

No. (4) 1·1-1·25 per cent carbon.
0·4 per cent manganese.
0·15-0·4 per cent silicon.

No. (5) 0·14 per cent carbon.
0·32 per cent manganese.
0·15 per cent nickel.

In order to establish the distribution of the lateral deformation (spread) over the width of the sheet, a screw with a pitch of 0·5 mm of No. 5 material was diametrally inserted into a wire of 9·85 mm diameter, also of No. 5 material. This sample was then flattened by rolling in a mill with rolls of 240 mm diameter, employing reductions of 13·2 per cent, 17·4 per cent and 27·5 per cent per pass respectively. The local spread over the width was found from the change in pitch of the screw. These tests showed that the largest specific spread obtains in the middle of the sheet where the deformation is greatest. The results of two typical tests are charted in Fig. 1. The influence of the rate of reduction per pass upon the magnitude of the residual stress was investigated on steel No. (1). For the purpose of this test, wire of 7·8 mm diameter was drawn to 7·4 mm diameter, corresponding to a reduction of 10 per cent.

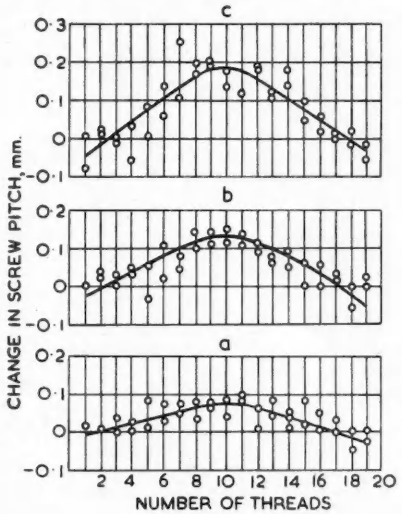

Fig. 1. **Distribution of lateral deformation over width of sheet.**
(a) Reduction of 13·2 per cent.
(b) „ „ 17·4 „ „
(c) „ „ 27·5 „ „

This wire was then flattened by rolling in a mill with rolls of 240 mm diameter, the successive reductions being 15·5 per cent, 28·7 per cent, 39·2 per cent and 49·4 per cent. The ultimate tensile stress as well as the percentage elongation and the residual stress of the rolled material were established as a function of the percentage deformation. The results are charted in Fig. 2 where it will be seen that strengthening of the metal by cold working is particularly pronounced in the first stages of working ; and as the ultimate tensile strength increases, the maximum residual stress is also increased.

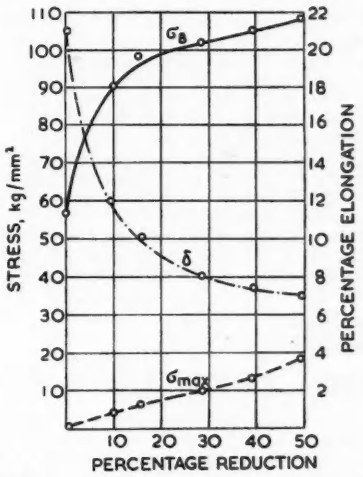

Fig. 2. **Maximum residual stress σ_{max}, ultimate tensile stress σ_B, and percentage elongation δ of steel sheet as a function of the reduction employed in rolling.**

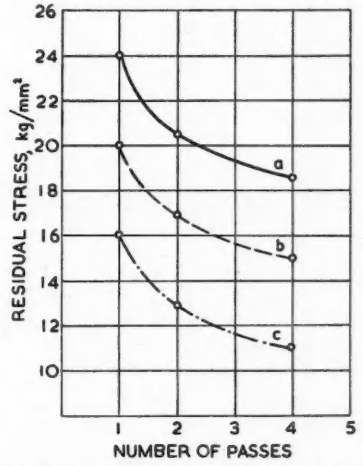

Fig. 3. **Maximum residual stress as a function of the number of roll passes.**
(a) No. 1 steel sheet, 3·75 mm thick.
(b) „ „ 4·90 „ „
(c) No. 2 „ „ 3·75 „ „

The influence of the original diameter of the wire from which the sheet is rolled was also investigated, wire of 7·4 mm, 9·5 mm and 12 mm diameter being used. It was found that for a given percentage reduction, the total lateral deformation increases with the original diameter. This also explains the influence of the original diameter upon the magnitude of the residual stress: The larger the original diameter, the greater the deformation, and, consequently, the smaller the residual stress.

In order to ascertain the influence of the number of passes employed in rolling the sheet, experiments were carried out on No. (1) steel, using rounds of 7·4 mm and 9·5 mm diameter respectively, and on No. (2) material using rounds of 7·4 mm diameter. The rounds of 7·4 mm were rolled into sheet of 3·75 mm thickness, one, two, and four passes with identical reductions being employed. The specimens of 9·5 mm diameter were rolled into sheet of 4·9 mm thickness. It was found that with a decreasing number of passes, the residual stress in the sheet increases as shown in Fig. 3. This behaviour is explained by the fact that by increasing the number of passes, the inequalities in deformation per pass decrease, with a corresponding diminution in residual stress.

The influence of the roll diameter upon the residual stress was also investigated. For this purpose, 1·4 mm diameter wire of material No. (3) was rolled into sheet between rolls of 240,150, and 90 mm diameter respectively, two and four passes with a total reduction of 64·3 per cent being employed in each case. Furthermore, 1·25 mm and 0·75 mm-diameter wire of material

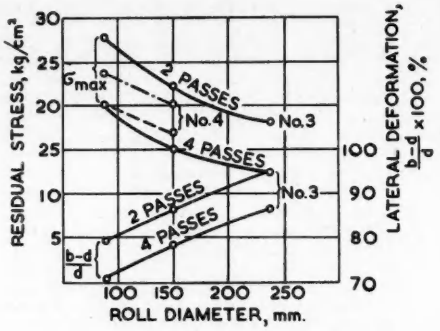

Fig. 4. **Maximum residual stress σ_{max} and lateral percentage deformation as a function of the roll diameter.**

No. (4) was rolled flat in four passes with a total reduction of 64 per cent. In all cases, the reduction per pass was kept constant. It was found that the distribution of residual stress over the cross-section of the sheet is very little influenced by the roll diameter. The maximum residual stress was observed to increase with smaller roll diameter, while the lateral deformation decreased as shown in Fig. 4. Such an increase in residual stress was also found to take place when rolling under tension. The application of grease to the contact surfaces during rolling considerably diminished the residual stress in the finished sheet.

HOLLAND

Proposal for Climb Requirements on a Rational Basis

By A. J. MARX. (From *De Ingenieur*, Vol. 60, No. 35, August 27, 1948, pp. L39-L44, 3 illustrations.)

1. INTRODUCTION

DURING the second Session of the Airworthiness Division of the ICAO (then PICAO) February-March, 1947, there appeared to be considerable opposition to the climb specifications laid down in the Airworthiness Standards, Practice and Procedure Recommendations Document, 2013 Air/69. In particular, the "V_s^2" law, giving the minimum required optimum rate of climb as a function of the square of the stalling speed, was considered by several member states to be inadequate as regards climb performance requirements from a safety standpoint, e.g. it gives too small a value for low stalling speeds and/or excessive values for high stalling speeds.

From the discussions it appeared that the reasons for choosing the V_s^2-law had only a poor theoretical foundation and were mainly based on experience with existing aeroplanes. This experience, however, only covered the range of low and intermediate stalling speeds, whereas almost no experience was yet available as to the high wing loadings and stalling speeds which will be introduced by designers in the near future.

2. BASIS FOR CLIMB SPECIFICATIONS

Climb specifications must ensure that an aeroplane, under certain specified conditions and of a given shape, shall have the ability to:

(a) maintain altitude (even under adverse weather conditions);

(b) clear obstacles during take-off and landing and when flying over mountainous terrain, clear meteorological obstacles, and change altitude in a reasonable time for traffic regulation purposes.

(c) carry out certain desirable manoeuvres, depending on the class of aeroplane under consideration.

To meet (a) it would be sufficient to specify a flat minimum value for the rate of climb, whereas for (b), the specification of a minimum angle of climb is the most rational solution. It is only in cases of exceptionally slow aircraft that an additional rate-of-climb specification might be necessary in order to guarantee a sufficient rate of climb for traffic purposes.

Item (c), however, raises more difficulties, because an exact definition of manoeuvrability and the extent of this requirement is difficult to formulate.

Doubtless, the most important factor here is the possibility of manoeuvring near the ground, especially in the case of take-off and landing (including balked landing), either with all engines working or with one or more engines cut out, to clear and/or avoid obstacles and turn around to make a new approach, when only a limited manoeuvring zone immediately surrounding the airport is available.

Since a specification corresponding to item (b) has to provide for the possibility of clearing more or less dense obstacles in the manoeuvring zone, the main object of item (*c*) should be to guarantee the possibility of avoiding isolated obstacles in that zone and to turn around before reaching higher obstacles beyond the manoeuvring zone.

It is, therefore, obvious that item (c) is mainly concerned with the lateral manoeuvrability.

Furthermore, it is known that every aeroplane with a certain power and wing loading has a certain minimum radius of turn in horizontal flight. As a measure of the lateral manoeuvrability, which is necessary for the following considerations, the value of this minimum radius of turn is chosen, considering that the smaller this radius, the better the manoeuvrability. The object of the present requirement is mainly to limit power and

wing loading to such an extent that dangerous combinations from a manoeuvrability standpoint are avoided.

It is rational that all aeroplanes requiring equal take-off distances must have such combinations of power and wing loading that an equal degree of manoeuvrability or, according to the above, an equal value of the minimum radius of turn is provided for, under the conditions specified by the near-ground operational standards.

The conclusions are that rational climb specifications should be based on the following principles:—

(i) A flat minimum value should be specified for the rate of climb.

(ii) Certain minimum values should be specified for the angle of climb, dependent on the flight conditions envisaged by the standards.

(iii) A climb specification should be laid down, covering the manoeuvring requirement that aeroplanes necessitating equal take-off distances shall have minimum radii of turn under the conditions specified by the near-ground operational standards.

3. CONSIDERATIONS UNDERLYING THE DRAFTING OF A CLIMB SPECIFICATION COVERING MANOEUVRABILITY

It may be assumed to be general knowledge that as a first approximation the take-off distance required may be considered as a function of the product of power loading ψ and wing-loading ϕ (c.f. ref. 1). Furthermore, an investigation based on ref. 2 has shown that this thesis may be expected to hold with an accuracy of about $\pm$ 15 per cent, as may be seen from Fig. 1, where, for twelve modern aeroplanes, the take-off distance is plotted on the product of power and wing loading in the case of all engines operating.

Principle (iii) may thus be interpreted as follows:—All aircraft having the same value of ϕ ψ shall have the same minimum radius of turn in horizontal flight.

When the minimum radius of turn R_m is expressed as a function of ϕ and ψ it is seen that variation of ϕ and ψ in such a manner that ϕ ψ is constant may produce variations in the minimum radius of turn of very considerable magnitude.

It appears impossible to stipulate that R_m should not vary with ϕ and ψ when ϕ ψ is constant. As an approximation, however, a condition may be laid down which limits the possible variation of R_m at constant values of ϕ ψ to an arbitrary extent. This means that a certain relation between ϕ and ψ is established.

When, on the other hand, the optimum rate of climb is expressed in terms of ϕ and ψ, introduction of the above-mentioned relation between ϕ and ψ creates a certain condition for the optimum rate of climb, which, by virtue of the relation between ϕ and the stalling speed, can be converted into a specification for optimum rate of climb as a function of the stalling speed.

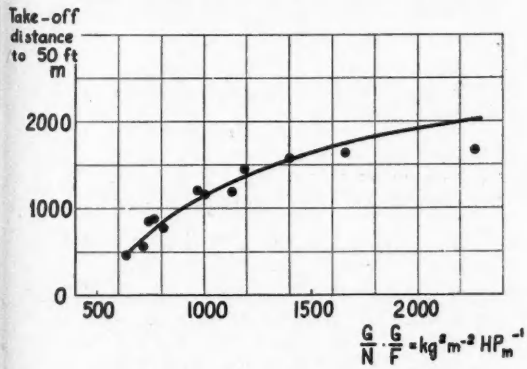

Fig. 1. **Take-off distance to 50 ft, all engines working, plotted on product of power and wing loading.**

4. CLIMB SPECIFICATION COVERING MANOEUVRABILITY

4. (1) *Minimum Radius of Turn in Horizontal Flight.*

For a horizontal turn the following relations are considered to be known:—

$$\frac{v_t^2}{gR} = \tan \varphi \quad .. \quad .. \quad (1)$$

$$\frac{G}{\cos \varphi} = \frac{1}{2} \rho v_t^2 F c_a \quad .. \quad .. \quad (2)$$

$$\eta N = \frac{1}{2} \rho v_t^3 F c_w \quad .. \quad .. \quad (3)$$

For convenience the following symbols are introduced:—

$$\phi = \frac{G}{F} \text{ (wing loading)} \quad .. \quad .. \quad (4)$$

$$\psi = \frac{G}{\eta N} \text{ (effective power loading)} \quad .. \quad (5)$$

Putting:

$$c_w = c_{wo} + a c_a^2 \quad .. \quad .. \quad (6)$$

the minimum radius of turn in horizontal flight can be expressed in terms of ϕ and ψ by

$$R_m^2 = \frac{1}{\rho^2 g^2} \frac{2^{12} a^4 \psi^4 \phi^4}{3^3 \rho^2 - 2^{10} a^3 c_{wo} \psi^4 \phi^2} \quad .. \quad (7)$$

when the c_a–value corresponding with this radius is smaller than the maximum value of c_a.

It may well be, however, that c_a, for the minimum radius of turn, exceeds the maximum c_a–value (c_{am}) for the aeroplane contour lines considered.

In this case R_m is given by (7a) where c_a is then equal to c_{am} and c_{wm} is the drag coefficient c_w corresponding to c_{am} viz.:—

$$R_m^2 = \frac{1}{\rho^2 g^2} \frac{4 \phi^2}{c_{am}^2 - \left(\frac{2}{\rho}\right)^{2/3} c_{wm}^{4/3} \psi^{4/3} \phi^{2/3}} . \quad (7a)$$

4. (2) *Minimum Radius of Turn R_m at ϕ ψ Constant.*

When in eq. (7) and (7a) the product ϕ ψ is kept constant, while ϕ and consequently ψ is varied, curves of R_m versus ϕ can be drawn.

These curves are shown in Fig. 2, viz., curves A corresponding to eq. (7) and curves B to eq. (7a). Where both curves touch, the c_a value is equal to c_{am}.

It appears that the curve of minimum radius of turn which can be obtained where there is a constant product of power and wing loading with varying wing loading is composed of two parts, viz., the left-hand part of A up to the value of ϕ at which c_a for the minimum radius of turn reaches c_{am}, and the right-hand part of B for c_a equal to c_{am}.

The ϕ value for which R_m reaches its minimum is

$$\phi = \frac{2^4}{3^{2/2}} \frac{c^2_{wm}}{\rho \; c^3_{am}} (\phi \; \psi)^2 \quad .. \quad (8)$$

4. (3) *Conditions Limiting the Variation of R_m.*

It is seen from Fig. 2 that, at $\phi\psi$ constant, the increase in R_m with decreasing ϕ from the value of ϕ for R_{mm} is very sharp. To attain as near as possible the object stated in 2 iii), some limiting condition for variation of R_m has to be introduced, which ensures

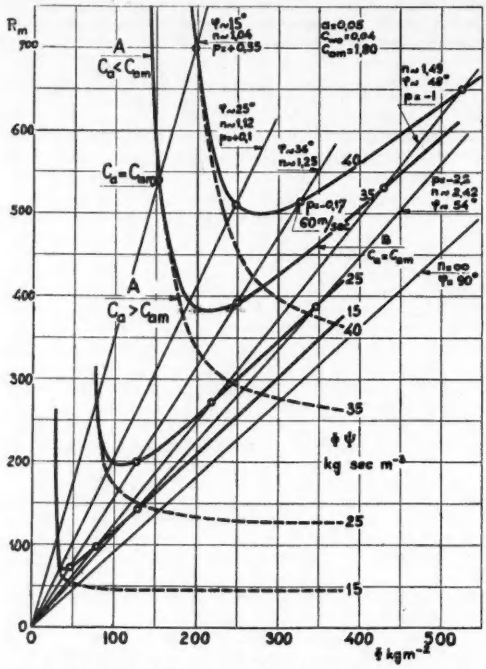

Fig. 2. **Minimum radius of turn plotted on wing loading for constant values of product of power and wing loading.**

that all aeroplanes having equal $\phi\ \psi$ values will have ϕ and corresponding ψ values only so much below or above ϕ from eq. (8) that the minimum radius of turn is only increased to a certain limited extent above the minimum R_m for that $\phi\ \psi$ value.

It is seen, furthermore, that with increasing ϕ the radius of turn increases more gradually.

It is, therefore, obvious that in the first place a downward limitation for ϕ is necessary. As to whether an upward limitation may be necessary, this will be considered later. Meanwhile, the following limitations will be introduced.

The value of ϕ at constant $\phi\ \psi$ shall be at most a certain percentage 100 p below or above the value ϕ for minimum R_m given by eq. (8). Numerical values for p will be considered later if necessary.

We, therefore, obtain the conditions:—

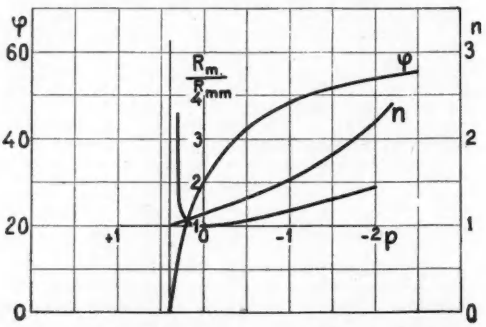

Fig. 3. **Variation of minimum radius of turn, angle of bank and load factor plotted on p for constant values of product of power and wing loading.**

$$\phi \geqslant (1-p)\frac{2^4}{3^{3/2}}\frac{c^2_{wm}}{\rho\ c^3_{am}}(\phi\ \psi)^2$$

where $p > 0$

and

$$\phi \leqslant (1-p)\frac{2^4}{3^{3/2}}\frac{c^2_{wm}}{\rho\ c^3_{am}}(\phi\ \psi)^2$$

where $p < 0$.

or

$$\frac{1}{\psi} \geqslant (1-p)^{1/2}\frac{4}{3^{3/4}\rho^{1/2}}\left(\frac{c^2_{wm}}{c^3_{am}}\right)^{1/2\ 1/2}\phi \quad .. \quad (9a)$$

where $p > 0$

and

$$\frac{1}{\psi} \leqslant (1-p)^{1/2}\frac{4}{3^{3/4}\rho^{1/2}}\left(\frac{c^2_{wm}}{c^3_{am}}\right)^{1/2\ 1/2}\phi \quad .. \quad (9b)$$

where $p < 0$.

The amount of increase in R_m for a certain value of p, is seen from

$$\frac{R_m}{R_{mm}} = \frac{(1-p)^{4/3}}{\left\{4(1-p)^{2/3}-3\right\}^{1/2}} \quad .. \quad (10)$$

Fig. 3 shows the relation between R_m/R_{mm} and p.

By choosing the limiting values p_1 and p_2 for p (p_1 positive and p_2 negative) in eq. (9), viz.:

$$p_1 > p > p_2 \quad .. \quad .. \quad (11)$$

according to eq. (10), we are able to limit the variation of the minimum radius of turn with varying ϕ at constant $\phi\ \psi$ value, expressed as a percentage of the smallest minimum radius of turn possible at that $\phi\ \psi$ value, to any degree required.

Figs. 2 and 3 show, furthermore, the values of the angle of bank φ and the load factor n corresponding to various limitations of wing loading (various p-values) at constant $\phi\ \psi$ values.

To summarize, conditions (9a) and (9b) for the relation between power loading and wing loading assure that all aeroplanes requiring take-off distances of approximately equal magnitude will, by a suitable choice of p, have approximately equal manoeuvrability characteristics.

4. (4) *Climb Performance.*

The basic formula for climb performance is

$$\eta N = {}^1/_2\,\rho\, v_c^3\, F c_w + Gw,$$

or

$$w = \frac{1}{\psi} - \frac{\rho}{2}\, v_c^3\, c_w\, \frac{1}{\phi}$$

It is easily seen that the condition for optimum rate of climb is given by

$$c_a^2 = \frac{3\,c_{wo}}{a} \quad .. \quad .. \quad (12)$$

Therefore, the optimum rate climb is

$$w_m = \frac{1}{\psi} - \frac{3^{5/8}\, a^{3/4}\, c_{wo}^{1/4}}{\rho^{1/2}\, 3^{3/4}}\phi^{1/2} \quad .. \quad (13)$$

In the event of the c_a value according to eq. (12) being larger than c_{am} the optimum rate of climb is given by

$$w_m = \frac{1}{\psi} - \left(\frac{2}{\rho}\right)^{1/2}\left(\frac{c^2_{wm}}{c^3_{am}}\right)^{1/2\ 1/2}\phi \quad .. \quad (13a)$$

4. (5) *Condition for R_m Coupled with Climb Performance and the Resulting Specification.*

By introducing eqs. (9a) and (9b) into eqs. (13) and (13a), conditions for climb performance are obtained, which are equivalent to eq. (9).

It is usual to express w_m in terms of the stalling speed v_{s1} which can be done by utilizing the equation

$$\phi^{1/2} = \left(\frac{\rho}{2}\right)^{1/2} c^{1.2}{}_{am} v_{s1} \quad .. \quad (14)$$

By introducing this equation as well as eq. (6), the climb requirement for manoeuvrability appears as

I: for $c^2{}_{am} > \dfrac{3c_{wo}}{a}$

$$w_m \geqslant 1{,}755 \left[\left(\frac{1-p}{2}\right)^{1/2} \frac{c_{wo} + ac^2{}_{am}}{c_{am}} - (a^3\, c_{wo}\, c^2{}_{am})^{1/4} \right] v_{s1} \quad .. \quad (14a)$$

where $p > 0$

$$w_m \leqslant 1{,}755 \left[\left(\frac{1-p}{2}\right)^{1/2} \frac{c_{wo} + ac^2{}_{am}}{c_{am}} - (a^3\, c_{wo}\, c^2{}_{am})^{1/4} \right] v_{s1} \quad .. \quad (14b)$$

where $p < 0$

II: for $c^2{}_{am} < 3\dfrac{c_{wo}}{a}$

$$w_m \geqslant \left[\left\{ 1{,}755 \left(\frac{1-p}{2}\right)^{1/2} - 1 \right\} \frac{c_{wo} + ac^2{}_{am}}{c_{am}} \right] v_{s1} \quad .. \quad (15a)$$

where $p > 0$

$$w_m \leqslant \left[\left\{ 1{,}755 \left(\frac{1-p}{2}\right)^{1/2} - 1 \right\} \frac{c_{wo} + ac^2{}_{am}}{c_{am}} \right] v_{s1} \quad .. \quad (15b)$$

where $p < 0$.

It is easily seen that eqs. (14) and (15) are identical for $c_{am}{}^2 = 3\, c_{wo}/a$.

The most important conclusion to be drawn from this result is:—

The rate of climb required to take care of manoeuvrability requirements is proportional to the stalling speed.

5. CLIMB SPECIFICATION RESULTING FROM PRINCIPLES GIVEN UNDER 2.

5. (1) *Specification of a Flat Minimum Value for w_m.*

The selection of numerical value w_f has to be based on experience regarding vertical components of downward air currents in the atmosphere, especially at airports in the neighbourhood of mountainous terrain.

5. (2) *Specification for a Minimum Angle of Climb.*

To be able to compare a specification for the angle of climb with the other specification, it is necessary to express it in terms of stalling speed. From considerations similar to those under 4 (4), the value of the optimum angle of climb could be derived. For convenience, however, this is not done and, instead of the optimum angle of climb (or the best gradient), the value of the gradient of the flight path at the optimum rate of climb is taken. The actual optimum gradient will, thus, be somewhat larger than calculated here; the difference, however, will be small.

According to this, we take for the optimum gradient w_m/v_c.

The optimum gradient of flight path has to be equal to or greater than a certain minimum allowable value q for the gradient. This leads to the condition

$$w_m \geqslant q \left(\frac{a}{3\, c_{wo}}\right)^{1/4} c_{am}{}^{1/2} v_{s1} \quad .. \quad .. \quad (16)$$

or

$$w_m \geqslant q\, A\, v_{s1} \quad .. \quad .. \quad .. \quad (17)$$

If, however, the c_a value for optimum rate of climb is greater than

$$c_{am} \left(\text{or } c^2{}_{am} < \frac{3\, c_{wo}}{a} \right), \text{ the value of } A = 1.$$

It is obvious that eq. (17) expresses w_m in the stalling speed at the same altitude as that to which w_m is related.

Thus, in general, the specification can be written:

$$w_m \geqslant K_1 v_{s1} \quad .. \quad .. \quad .. \quad (18)$$

5. (3) *Specification for Manoeuvrability.*

According to 4 (5), this can be formulated as:

$$w_m \geqslant K_2 v_{s1} \quad .. \quad .. \quad .. \quad (19a)$$

for $p > 0$

and

$$w_m \leqslant K_2 v_{s1} \quad .. \quad .. \quad .. \quad (19b)$$

for $p < 0$

6. CONCLUSIONS

The most important facts to be noted from the above are:

(1) The specification for gradient of flight path will, in general, dominate the specification for manoeuvrability resulting from the lower limit on the wing loading.

(2) Though dependent on the variation of manoeuvrability which is considered acceptable, it is possible that too severe a specification for the gradient of flight path might impair the manoeuvrability.

Furthermore, comparison with the existing requirements gives rise to the following remarks; they should, however, not be considered as a complete criticism, but simply as an indication of some outstanding conclusions.

(3) The existing ICAO standard (Doc 2013) for " en route " climb, all engines working, is in agreement with the above results for a gradient of flight path of about 0·5.

(4) The existing specification for take-off and approach, one engine being cut out, must certainly be considered inadequate for stalling speeds below 140 km/h (87 mph). For very high stalling speeds, the specification is unnecessarily severe.

(5) The existing specification for " en route " climb, one engine being cut out, must probably be considered inadequate for stalling speeds below 250 to 125 km/h (160 to 80 mph), depending on the take-off weight, and too severe for very high stalling speeds.

(6) The existing specification for balked landing must be considered rather servere, and there might even be a possibility of the manoeuvrability being impaired for stalling speeds higher than about 220 km/h (140 mph).

(7) Notations

G aircraft weight (kg)

N total horse-power of aircraft (kg m sec^{-1}) (cruising, take-off, one engine cut out, etc., depending on flight condition considered)

η	propeller efficiency
F	wing area (m²)
ϕ	G/F wing loading (kg m⁻²)
ψ	$G/\eta N$ " effective " power loading (sec m⁻¹)
v_t	true airspeed in horizontal turn (m sec⁻¹)
v_c	true airspeed in straight climb (m sec⁻¹)
v_{s1}	stalling speed in a certain aeroplane configuration and at a certain altitude (m sec⁻¹)
w	rate of climb (m sec⁻¹)
w_m	maximum rate of climb (m sec⁻¹)
R	radius of horizontal turn (m)
R_m	minimum radius of horizontal turn at a certain power and wing loading (m)
R_{mm}	absolute minimum radius of horizontal turn possible when varying power and wing loading under certain conditions assumed in this report (m)
c_a	lift coefficient
c_{am}	maximum lift coefficient
c_w	drag coefficient
c_{wm}	drag coefficient at maximum lift coefficient
c_{wo}	drag coefficient at zero lift coefficient
a	parameter in the equation $c_w = c_{wo} + ac_a^2$
ρ	air density (kg sec² m⁻¹) taken as 0·125
g	acceleration due to gravity (m sec⁻²) taken as 9·81
φ	angle of bank
p	a constant defined under 4 (3)
q	gradient of flight path in straight climb.
n	load factor
A, K_1, K_2	constants defined under 5 (2) and 5 (3).

REFERENCES

(1) WARNER, E. P.: Post War Transport Aircraft. *Interavia* No. 878, July 29, 1943.

(2) LUCASSEN, L. R.: N.L.L.-report V. 1411 (not yet published).

RUSSIA

Method of Testing Fatigue of Steel Samples at High Temperatures

By M. F. SICHIKOV and Z. D. VISHNEVECKY. (From *Zavodskaya Laboratoria*, No. 1, 1948, pp. 86-91, 5 illustrations).

MEASUREMENTS have been taken at the Ural Turbine Factory on a Schenk type fatigue tester, but the methods of testing were developed and improved by the Turbine Factory Laboratory. Fatigue tests were carried out for the condition of bending of cylindrical test pieces at temperatures up to 600° C while revolving at speeds of 5000 rpm and above. The test pieces were heated in an electric furnace consisting of four sections, each with independent current regulation (see Fig. 1). The two inner bearings are protected from the heat of the furnace by asbestos shields and it was found that the heat dissipation in the bearings is better when the speed of rotation is higher.

One of the main difficulties encountered was the method of temperature measurement. A thermo-couple was used, and while it is desirable to attach it to the test piece, it was found that this involved serious complications, as slip-rings were required to take the current off the rotating part. With the low e.m.f.'s involved, inaccuracies occur due to variation of contact resistance between slip-ring and brush, particularly when both parts become worn. For these reasons, the temperature in the space between the furnace wall and test piece was measured and compared with the temperature of the test piece itself by means of calibration curves.

To obtain accurate and reliable results, it is important to have the test piece heated evenly over its whole length and this is obtained by raising the temperature of the outer sections of the furnace to some extent above that of the inner sections. The cylindrical test pieces used were of standard size and shape, in contrast to the rather complicated shape recommended by the makers of the testers. Apart from the difficulty of producing large numbers of these testers, it was considered that their construction had an inherent fault, the cross-section being smallest in the centre of the test piece so that the location of the break is, therefore, predetermined. In order to shorten the duration of tests, it is often convenient to calculate the fatigue point and it is found that for steel with high chromium content and certain other alloy steels at high temperatures the well-known formula of Goudremon and Mailänder still applies.

$$\sigma_w = 0{\cdot}25\,(\sigma_B + \sigma_s) + 5\ \text{kg/mm}^2$$

where the values of σ_B and σ_s must, of course, be those applicable to the test temperature.

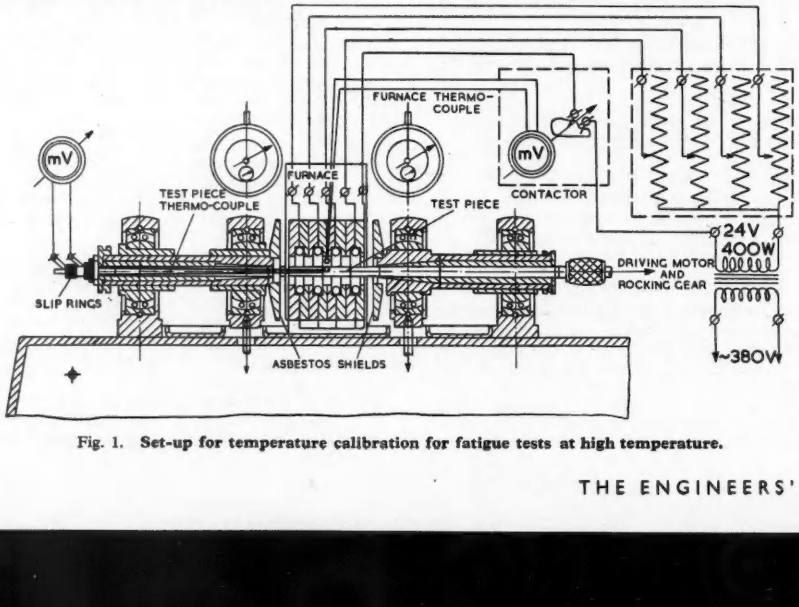

Fig. 1. **Set-up for temperature calibration for fatigue tests at high temperature.**

Application of Hydraulic Calculations to the Design of Pouring Gates for Castings

By J. KIESWETTER. (From *Hutnické Listy*, Vol. 3, No. 6, June, 1948, pp. 165-170, 11 illustrations.)

CASTING is basically a hydraulic process, so that, by hydraulic analysis of the design of pouring gates, the number of defective castings can be considerably reduced.

To obtain favourable flow conditions of the molten metal, it is necessary to choose an appropriate pouring system and to determine favourable shapes and dimensions of the individual passages of the pouring gates.

The basic assumptions adopted in the usual hydraulic calculations are as follows: continuity of flow, homogeneity of the flowing medium, non-porosity of the walls surrounding the medium, and uniformity of flow along its entire path. These conditions are not fulfilled in the casting process and it is necessary, therefore, to adapt the hydraulic calculations to the requirements of the casting process.

The following well-known hydraulic basic equations are applied:—

The law of continuity of flow $Q = Fc$ .. (1)

where Q is the flow volume, F its cross-section, and c the flow velocity.

The interrelation between static and dynamic energy of the fluid is expressed by

$$\frac{c^2}{2g} = H \quad .. \quad .. \quad (2)$$

where H is the height of the fluid column which causes the fluid to flow at a velocity c and

$$p = \gamma H \quad .. \quad .. \quad (3)$$

where γ is the specific weight of the fluid.

The condition of flow continuity demands that the fluid in motion shall be prevented from mixing with other elements, such as air, gases, etc. For this reason, it is necessary for the walls to be gas-tight, but the walls of moulds are porous, and mixture of the molten metal with gases is intensified in many cases by turbulence. Viscosity and high surface stresses prevent penetration of the molten metal through the pores of the mould, but air and gases easily penetrate to the interior of the mould, particularly because the pores of the mould material are filled with gases, and additional gases are generated as a result of the burning of combustible admixtures with the sand.

One way of eliminating absorption of gas by the flow of molten metal is to create favourable flow conditions by suitable design of the pouring gates. It is desirable to obtain a laminar flow in the pouring gates, but in most cases not only the dimensions of the pouring gates, but also the flow speed are such that the flow is turbulent.

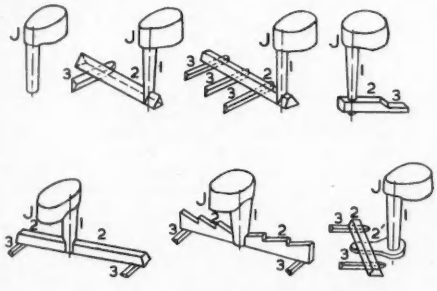

Fig. 1. **Various types of pouring gates.**
J = feed head, 1 = downgate, 2 = main channel, 3 = ingate.

A pouring gate of 40 mm dia. and the usual gradient will cause the flow to be turbulent, but a laminar flow can be obtained by substituting 18 channels of 10 mm dia. each, as is the case with light alloy casting work.

The unfavourable effects of turbulent flow also result in an increase of the vacuum (decrease of the pressure) in the flow of the molten metal, caused by the hydraulic conditions of the flow. If disturbances caused by the penetration of air and gases into the flow of molten metal are to be prevented, then it is necessary to design the flow cross-sections in such a way that the pressure in the flow shall be higher than the ambient atmospheric pressure.

There are various types of pouring gates, and some of the systems in current use are represented in Fig. 1. Such gating systems are composed of a vertical section, the downgate (1), a connecting section, namely, the main channel (2), and the inflow opening, the ingate (3) which leads into the mould.

To elucidate the theoretical conditions of correct design of gating systems, let us investigate some cases of flow of fluids from containers through orifices. Only the steady state is investigated and the starting conditions are not taken into consideration.

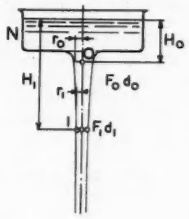

Fig. 2.
Outflow from a container into the open air.

Disregarding losses, we obtain for the point O (see Fig. 2) of the cross-section F_0 of the opening, situated at a depth H_0 below the surface level of the fluid, the speed of flow

$$c_0 = \sqrt{2gH_0} \quad .. \quad .. \quad (4)$$

and the quantity of fluid per second

$$Q_0 = F_0 c_0 \quad .. \quad .. \quad .. \quad (5)$$

and for a given value of Q:

$$F_0 = Q/c_0 = Q/\sqrt{2gH_0} \quad .. \quad .. \quad (6)$$

It is assumed that the liquid level $O - O$ remains constant during the steady-state conditions of the flow.

The flow speed at the point 1 is

$$c_1 = \sqrt{2gH_1} \quad .. \quad .. \quad (7)$$

and the corresponding cross-section

$$F_1 = Q/\sqrt{2gH_1} \quad .. \quad .. \quad (8)$$

and it is obvious from the above equations that $F_1 < F_0$.

The relation between F and H follows from:—

$$F_0 c_0 = F_1 c_1 = F_0\sqrt{2gH_0} = F_1\sqrt{2gH_1} \quad .. \quad (9)$$

or $$F_0/F_1 = H_1/H_0$$

and $$F\sqrt{H} = K = \text{const}, F = K/\sqrt{H} \quad .. \quad (10)$$

where $$K = Q/\sqrt{2g} \text{ and } HF^2 = K^2 \quad .. \quad (11)$$

For a circular cross-section we obtain from eq. (10):

$$r^2 = \frac{1}{\pi\sqrt{H}}\,\frac{Q}{\sqrt{2g}} \quad .. \quad .. \quad (12)$$

and $$r^4 = \frac{1}{H}\,\frac{Q^2}{\pi^2 2g} = \frac{1}{H}\,K' \quad .. \quad (13)$$

where $$K' = \frac{Q^2}{2g} = Hr^4 \quad .. \quad .. \quad .. \quad (14)$$

The cross-section available to the molten metal for any given point below the surface should be at least as large as that obtained by the above formulae. A pressure above atmospheric in the liquid flow is favourable and can be obtained by making the cross-section for the flow larger than the value obtained according to this method, but the narrowest (effective) cross-section must be that obtained by calculation.

For gating systems where there is a considerable loss of speed along the walls, the speed at the narrowest cross-section is calculated by taking into consideration the various speeds in the different sections of the flow path. The basic equation for this calculation is :

$$H_c = \frac{c^2}{2g}\left[(1 + \Sigma\xi) + \Sigma\left(\frac{F}{F_x}\right)^2 \Sigma\xi_x\right] + h$$

$$= \frac{c^2}{2g}\left[(I) + (II)\right] + h \quad .. \quad .. \quad (15)$$

where H_c is the total head of the fluid metal, ξ and ξ_x are coefficients which characterize the losses due to changes of the size and shape of the cross-section and those due to change of direction of the flow and friction on the walls. h is the head of fluid required for driving out the air and gases from the mould during the casting process. The term $I = 1 + \Sigma\xi$ of the equation is the part of the equation representing the relation for the section with the narrowest cross-section F, the term $II = \Sigma(F/F_x)^2\,\Sigma\xi_x$ is the part of the equation relating to the cross-sections $F_x > F$. The coefficient ξ is given in text books on hydraulics.

The practical solution is to calculate the hydraulic conditions for a large number and large variety of sizes of standardized gating systems and to tabulate the results obtained in the form of charts for distribution to foundries.

A detailed description of these calculations is outside the scope of this paper, but it is interesting to compare the pressure characteristics of some of the numerous types of gating systems with one another and, in turn, to compare these with the conditions of a free flow.

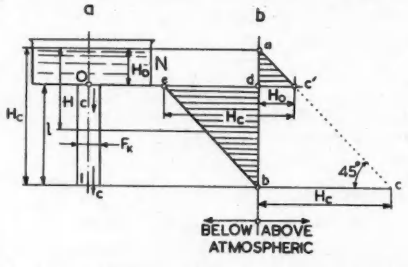

Fig. 3a. **Outflow from a container through a vertical channel of uniform cross-section.**

Fig. 3b. **Pressure diagram for a flow produced only by potential energy.**

The simplest gating system is that having a vertical path of constant cross-section emerging from the bottom of a container, which represents the feeder load. If the stream were to issue into the open, and if the bottom of the tube in which the flow takes place were not submerged below the bottom liquid level (Fig. 3a), the stream would not fill the whole cross-section and part of the flow adhering to the wall would separate from the rest. The flow speeds would increase with the depth, corresponding to the value obtained from eq. (7).

If the bottom end of the vertical channel is submerged below the bottom level of the liquid, the flow will fill the whole cross-section, and owing to constant speed throughout the vertical channel, the characteristic of the pressure will be such as is represented in Fig. 3b. The speed and pressures are functions of the total head H_c and we obtain for the speed at the outflow cross-section

$$c = \sqrt{2g\,Hc}$$

As the cross-section is constant, the flow speed will also be constant from point O to point 1 (Fig. 3). If the outflow end were to be closed at the point 1, the flow speed would be zero and the static pressure at any point would be proportional to its depth below the surface of the liquid level, line *a-c* in Fig. 3b. If the outflow opening is opened at point 1 the speed of flow (steady state) throughout the vertical column will be c and the pressure throughout this column will drop below the ambient atmospheric pressure. The pressure in the container will be above atmospheric, represented by the line *a-c'* in Fig. 3b, and in the vertical column there will be a sub-atmospheric pressure, represented by the line *e-b* in Fig. 3b. The lowest pressure will be at O with the value $H_c - H_0$ below atmospheric pressure. If losses were taken into consideration, the outflow speed would be represented by the equation:

$$H_c = \frac{c^2}{2g}(1 + \xi_c + \xi_a) \quad .. \quad .. \quad (16)$$

where ξ_c is the loss coefficient of the outflow orifice of the container, and ξ_a is the loss coefficient of friction on the walls. The pressure characteristic changes for this case, and is wholly unsuitable for gating systems.

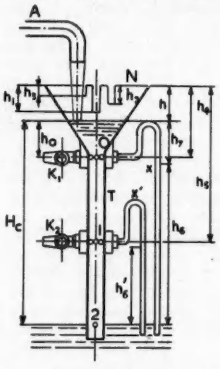

Fig. 4. **Model for experimental determination of sub-atmospheric pressure in a vertical channel of uniform cross-section.**

To confirm these theoretically obtained results, a metal model was made (Fig. 4) and the experiments were carried out with water. The heights of the water columns in the piezometric tubes connected to the points O and 1 of the model were h_6 and h_6'. This confirmed that sub-atmospheric pressure does occur in the vertical tube and that its characteristic is linear. When the cocks K_1 and K_2 were opened, air was sucked in, which escaped through the outflow end, in the form of air bubbles, below the lower water level.

Experiments with water give similar results to those obtained with molten metal, and the viscosities of both liquids have to be taken into consideration when comparing the results.

The viscosity of molten cast iron at 1400° C is $\nu_i = 0{\cdot}28 \times 10^{-6}$ m²/sec, that of water at 20° C is $\nu_w = 1{\cdot}01 \times 10^{-6}$ m²/sec.

The basic difference between the two media is that their surface tensions differ greatly, and this manifests itself in the fact that molten cast iron does not adhere to the walls, whereas water does. This affects the boundary layer and is already taken into consideration by the loss coefficient.

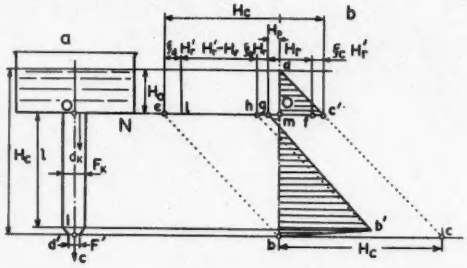

Fig. 5a. **Outflow from a vessel through a vertical channel with the cross-section constricted at the outflow end.**

Fig. 5b. **Pressure characteristic taking account of losses.**

If the outflow opening of the channel is made narrower (Fig. 5), there will be a maximum speed of flow c in the narrowest cross-section at point 1, whereas the flow speed c_k in the channel above this point would be lower,

$$c_k = c\,F/F_k \qquad .. \qquad .. \qquad (17)$$

For an outflow into the open air, there will be the following losses which influence the speed c :—

(1) Losses due to the inflow from the container to the channel at O, loss coefficient ξ_c,
(2) friction in the channel O — 1, loss coefficient ξ_a,
(3) resistance at the outflow point, loss coefficient ξ_d.

The basic equations for determining the flow speed are:

$$H_c = \frac{c^2}{2g}(1 + \xi_d) + \frac{c_k^2}{2g}(\xi_c + \xi_a)$$

$$= \frac{c^2}{2g}\left[(1 + \xi_d) + \left(\frac{F}{F_k}\right)^2(\xi_c + \xi_a)\right] \quad .. \quad (18)$$

$$c_k = \frac{F}{F_k}\,c \quad \text{and for} \quad \frac{c_k^2}{2g} = H_r;\ \frac{c^2}{2g} = H_r' \quad .. \quad (19)$$

We obtain $H_c = H_r'(1 + \xi_d) + H_r(\xi_c + \xi_a)$ .. (20)

It can be seen from the pressure diagram, Fig. 5b, that making the outflow cross-section at its bottom end narrower is a suitable method of reducing the vacuum in the vertical flow. The pressure at O is smaller than the atmospheric pressure by the value

$$H_p = H_r(1 + \xi_c) - H_0 \qquad .. \qquad .. \qquad (21)$$

To eliminate the sub-atmospheric pressure entirely, i.e. for $H_p = 0$

$$H_r = \frac{c_k^2}{2g} = H_0\,\frac{1}{1 + \xi} \qquad .. \qquad .. \qquad (22)$$

and the flow cross-section of the channel F_k must be designed accordingly, or the depth of the liquid in the container must be equal or larger than a–m (Fig. 5b).

A further example is the pressure characteristic in a horizontal outflow duct of constant cross-section, through which a liquid flows from a container into the open air. The total head H_c consists of the fluid column in the container. The theoretical value of the flow speed in the outflow duct is:

$$H_c = \frac{c^2}{2g} \qquad .. \qquad .. \qquad .. \qquad (23)$$

and taking into consideration the losses:

$$H_c = \frac{c_z^2}{2g}(1 + \xi_c + \xi_a) \qquad .. \qquad (24)$$

From this we obtain:

$$c_z = \sqrt{2g\,H_c\,\frac{1}{1 + \xi_c + \xi_a}} = c\,\sqrt{\frac{1}{1 + \xi_c + \xi_1}} = \mu c \qquad (25)$$

The pressure in the outflow duct O–1 depends on the resistance in the duct and its characteristic is given by a straight line.

If the outflow end of the duct is narrowed, the pressure inside the duct would increase by the value of the pressure drop in the narrow outflow end h''':

$$h''' = \frac{c^2 - c_k^2}{2g} + \frac{c^2}{2g}\xi_d = \frac{c_k^2}{2g}(1 + \xi) - \frac{c_k^2}{2g}$$

$$= \frac{c^2}{2g}\left[1 + \xi_d - \left(\frac{F}{F_k}\right)^2\right] \qquad (26)$$

Let us examine the case of a variable outflow cross-section with a vertical section, followed by horizontal sections; such an arrangement is frequent in moulds (Fig. 6). The maximum speed will again occur where the cross-section is smallest, and this speed is obtained by using the basic equation (15).

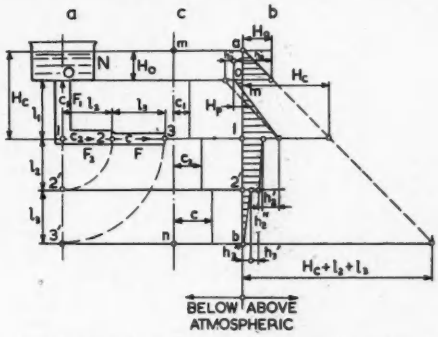

Fig. 6a. **Outflow through a vertical channel connected to a horizontal channel of variable cross-section.**

Fig. 6b. **Pressure characteristic of flow.**

Fig. 6c. **Speed characteristic of flow.**

The flow speed diagram is represented in Fig. 6c, the pressure diagram in Fig. 6b; the zero axes of both diagrams are drawn on a vertical line to improve the clarity of the figure. There is a certain vacuum at O, which can be eliminated either by increasing the cross-section of the vertical part of the flow, or by increasing the depth of the fluid in the container to the value a–m.

In some cases, the vacuum in the vertical parts is reduced by interrupting it to allow the flow at the interruption point to form a free flow (a flow in the open air). Such an arrangement is often made when casting into large moulds of considerable height, e.g. for casting ingots (Fig. 7). N_1 represents the casting ladle; the outflow opening is in the bottom and the free stream emerging from it flows into a wider channel K, in which a new, free, surface level O'–O' is formed. From this wider cross-section the fluid flows, under the pressure developed by the oncoming stream at the point 1 of the level O'–O', to the mould N_2, and the

static pressure will be H^+ (which can also be a negative value). The pressure developed by the advance of the free stream is:

$$h_p = \frac{c' - c_1}{g} c_1 \quad .. \quad .. \quad (27)$$

where c' is the speed of the issuing stream, and c_1 is the speed in the wider channel K.

The pressure characteristic obtained from calculations of this flow system is represented in Fig. 7b. It can be seen that the pressure characteristic is improved and vacuum is eliminated. A further advantage of this system is that the casting conditions at the beginning, and throughout the duration of the casting process can be suitably arranged to obtain only a small variation of the flow speed, in spite of the large differences in the surface level in high moulds at the beginning and end of the casting process.

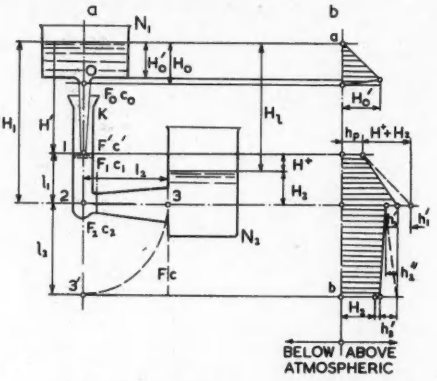

Fig. 7a. **Free outflow from a vessel N_1 into the adjustment channel K of the pouring system 1-2-3 for filling vessel N_2 which represents the mould.**

Fig. 7b. **Pressure characteristic in the vessel N_1, in the open air flow, and in the flow system for the liquid levels H_1 and H.**

The few examples of flow systems described in this paper demonstrate the basic principle of the theoretical analysis of gating systems. For practical purposes it will be necessary to analyse a large series of gating systems and find optimum designs for them. These designs will have to be classified, standardized and made available in tables and instruction books. Before doing this, it will be necessary to check the results obtained theoretically by experiments with water and molten metal.

Progress in Separation Methods

By P. KLINGER and W. KOCH. (From *Stahl und Eisen, Germany*, Vol. 68, No. 19/20, September 9, 1948, pp. 321-333, 17 illustrations).

NOWADAYS, it is important to know not only the chemical composition of a steel, but also its structural details, their composition, form and distribution. Chemical separation methods isolate these details, whether inclusions or steel components, without modifying them. The authors have adapted existing separation methods and have obtained satisfactory extraction of oxidic inclusions from alloyed and unalloyed steels. By their method, metallic parts of the steel are first electrolytically dissolved and a powdery anodic residue is obtained consisting of carbides, sulphides, nitrides, and oxides. The oxides are then separated from the rest by the chlorine method. For the electrolysis, anode (steel sample) and cathode (copper wire mesh) are separated by a diaphragm. The anode space is filled with a 5 to 15 per cent solution of nacitrate to which fluorides may be added with advantage, the cathode space with Cubromide. Highly alloyed (chromium) steels offer difficulties when forming passive zones at the steel surface. However, if the poles are reversed the surface can be activated again by the action of hydrogen forming at the surface. A trapezoidal current is therefore superimposed on d.c. so that anodic treatment is interrupted periodically by short intervals of pole reversal and re-activation of the specimen surface. Since electrolytic treatment dissolves all the metallic parts, the subsequent chlorine treatment of the anode residue can be undertaken at relatively low temperatures (200 to 250° C) and local overheating due to exothermic reactions can be avoided. Moreover, the treatment has to remove only small amounts of powdery residue and can be done in still chlorine gas so that the reaction is slower and less severe on the oxide inclusions. The chlorides formed are sublimated in vacuo*. Extracted oxide inclusions consist of a fine powder, partly coloured, partly colourless, and their structure and external shape, if seen under the microscope, compares well with that found in metallographic investigation. Since extracted oxide inclusions are mostly transparent, their composition can be determined by diffraction.

Oxide inclusions extracted from rimmed steels can be observed down to smallest particle sizes, some particles being only visible under the electron-microscope (16,000 magn.). It can be concluded that the method employed succeeds in extracting practically all oxide inclusions, that the finest inclusions must have segregated after solidification, and that, since at least for rimmed steels the amount determined from analysis is greater than that found from extracted inclusions, some oxygen probably remains "dissolved" in the steel. In completely de-oxidized steels, the oxide inclusions have been formed during the melt and from composition and concentration of the extracted inclusions, the different stages of the de-oxidation process can be deduced. The behaviour of inclusions during the working of steel can also be shown by inclusions extracted before and after working. Crystallized inclusions are not deformed during working unless they have been softened by heating before forging. Undercooled, glass-like inclusions, however, can be drawn out to fibres or very thin, frequently disrupted, films. If crystalline inclusions are surrounded by glass-like envelopes of a similar composition, the envelope is deformed and torn off during working but the crystalline centre remains undeformed. That the crystallization of inclusions depends on the rate of cooling can also be shown by the crystallic structure of the extracted inclusions, as observed under polarized light†.

Carbides can be extracted, by the same electrolytic method, from alloyed and un-alloyed steels, even when they are extremely finely distributed. The difficulties the metallographic method presents for the investigation of very fine carbides can be avoided and very clear pictures of separated fine carbides are obtained under the electron-microscope. Comparison with metallographic investigation of coarser carbides shows the correctness of the picture obtained by the extraction method. This method, in conjunction with electron-microscopic and X-ray investigations, therefore offers new possibilities of determining the structural composition of steels.

*A schematic sketch of the chlorine-vacuum apparatus is given in the original paper.—*Ed., E.D.*

†A tertiary diagram showing shape, colour and plasticity of inclusions as a function of their composition is given for well de-oxidized steel.—*Ed., E.D.*

Stresses in Transversely Bored Shafts Subjected to Torsional Loading

By G. SEEGER. (From *Die Technik*, Vol. 3, No. 7, July, 1948, pp. 309-311, 5 illustrations.)

THE shafts considered in this report are circular-section shafts with a hole perpendicular to the shaft axis and passing through the centre of the shaft cross-section, as shown in Fig. 1.

1. CALCULATION OF NOMINAL STRESS

If the diameter d of the hole is small relatively to the shaft diameter D, the polar moment of inertia of the section can be approximated by the expression

$$I_{\text{hollow}} \equiv I_h \cong \frac{\pi D^4}{32} - \frac{Dd^3 + dD^3}{12} \quad .. \quad .. \quad (1)$$

In this approximation the moment of inertia of a rectangle of sides D and d is subtracted from the moment of inertia of a solid circular section. The accurate formula, however, takes account of the fact that the circular section is weakened, not by a rectangular area, but by a somewhat smaller area bounded by circular arcs on the smaller sides. Eq. (1), therefore, gives a moment of inertia which is too small, and the discrepancy increases with increasing values of the hole diameter d.

If the circular shape of the sides is taken into account in the area which is subtracted from the solid section, the exact expression for the moment of inertia is obtained:

$$I_h = \frac{\pi D^4}{32}\left(1 - \frac{2}{\pi}\ \text{arc sin}\ \frac{d}{D}\right) - \frac{d}{48}\sqrt{D^2 - d^2}\,(2d^2 + D^2) \quad .. \quad (2)$$

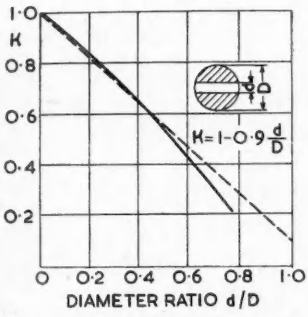

Fig. 1. **The flexibility coefficient κ as a function of the diameter ratio d/D.**

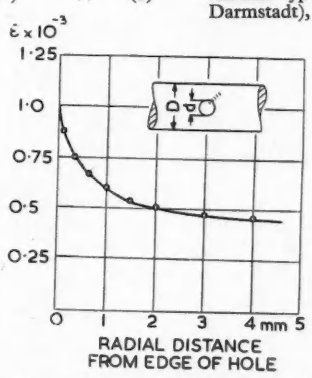

Fig. 2. **Decrease of strain with radial distance from edge of hole on a torsion shaft with a transverse hole 5 mm in diameter.**

The arc sine function can be replaced by a power series which converges fairly rapidly, so that even with the first two or three terms an accuracy of 0·5 per cent is obtained. The equation then becomes

$$I_h \cong \frac{\pi D^4}{32} - \frac{D^4}{16}\left(\frac{d}{D} + \frac{1}{6}\frac{d^3}{D^3} + \frac{3}{40}\frac{d^5}{D^5}\right) - \frac{d}{48}\sqrt{D^2 - d^2}\,(2d^2 + D^2) \quad .. \quad (3)$$

If $I_s = \pi D^4/32$ = moment of inertia of the solid section, and $I_h/I_s \equiv \kappa$, then the polar moment of inertia of the shaft with the transverse hole, as well as the corresponding sectional modulus Z_h, and the nominal shear stress τ_n can be obtained by means of the relations:

$$\left.\begin{aligned} I_h &= \kappa I_s = \kappa\pi D^4/32 \\ Z_h &= \kappa Z_s = \kappa\pi D^3/16 \\ \tau_n &= \tau_s/\kappa = 16M_t/(\pi D^3\kappa) \end{aligned}\right\} \quad .. \quad (4)$$

The coefficient κ is shown in Fig. 1 as a function of the diameter ratio d/D. The solid line gives the exact value of the moment of inertia calculated according to eqs. (2) and (3). For all holes for which $d < 0{\cdot}5D$, the κ-curve can be replaced by a straight line

$$\kappa = 1 - (0{\cdot}9\ d/D),$$

so that graphical determination will not be necessary. The equations (4) then become

$$\left.\begin{aligned} I_h &\cong (1 - 0{\cdot}9\ d/D)I_s \\ Z_h &\cong (1 - 0{\cdot}9\ d/D)Z_s \\ \tau_{nh} &\cong \tau_s/(1 - 0{\cdot}9\ d/D) \end{aligned}\right\} \quad .. \quad .. \quad (5)$$

These simple equations give results differing by less than 1 per cent from the values obtained by means of the exact eq. (2).

2. STRAIN MEASUREMENTS FOR THE DETERMINATION OF THE FORM FACTOR

The stress peak at the edge of the hole or in its immediate vicinity is usually determined by means of a form factor α_K which gives the ratio of the maximum effective stress to the nominal calculated stress: $\alpha_K = \tau_{\max}/\tau_{nh}$.

The maximum stresses were determined on five test specimens of duralumin (Al-Cu-Mg) by means of Askania-type precision strain gauges (model MPA Darmstadt), with a gauge length of 2 mm, and by means of Granacher strain gauges with a 5 mm gauge length. The test specimens had diameters of 39·5 or 40 mm and hole diameters varying from 5·1 mm to 30 mm.

Preliminary tests showed that for small d/D ratios the maximum strain is at the point of contact of the 45-degree tangent, while for larger d/D values the maximum strain will be displaced towards the weakest cross-section. The radial decrease of strain was measured beginning from the maximum strain position at the 45-degree point on the edge of the hole, with the strain gauge at 45 degrees but placed at increasing distances from the hole centre. The measurements were made at points relatively close to one another; in the neighbourhood of the hole the measurement points were only 0·2 mm apart. The position of the gauge was determined by means of an optical micrometer giving the distance between the gauge indentation and the hole. The results for a given specimen are shown in Fig. 2.

The results obtained from careful measurements on all five specimens are represented in Fig. 3, which shows that the form factor $\alpha_K = \tau_{\max}/\tau_{nh}$ increases from 2·3 to 3·0 for d/D varying from 0·05 to 0·75. For most cases the form factor $\alpha_K = 2{\cdot}7$ can be used for calculation of maximum stresses. The form factor $\alpha_K = 4{\cdot}0$ obtained theoretically by other investigators is based on the consideration of the plane state of stress in an infinitely large, perforated disk. Tests carried out by the author of this article have shown that the form factor $\alpha_K = 4{\cdot}0$ is a limiting value for hollow shafts, which is only reached when the wall thickness

of the hollow shaft is reduced to such an extent that it becomes a thin tube with a transverse hole perpendicular to the tube axis.

If the form factor α_K is related to the nominal stress τ_{ns} of the full solid section instead of the stress τ_{nh} of the hollow section, the dotted curve shown in Fig. 3 is obtained, which rises asymptotically for large values of d/D.

3. TESTS TO DETERMINE STATIC AND DYNAMIC STRENGTH

To determine the effect of the transverse hole on the yield point and the fatigue strength of shafts a series of static and dynamic tests were carried out.

For yield point determination the specimens used were bars 60 cm long and 30 and 40 mm in diameter, made of annealed carbon steels with ultimate tensile strengths of 80 and 85 kg/mm². The yield point was determined optically and the variation of yield strength with the diameter ratio d/D is shown in Fig. 4. It is apparent from this figure that the yield strength drops appreciably for values of d/D greater than 0·3. The chain-dotted line at the bottom of the figure gives the ratio of the yield strength of the solid section to that of the hollow section as a function of d/D, and shows that the yield strength drops to 75 per cent of its original value when $d/D = 0{\cdot}7$.

The torsional fatigue strength was determined using test bars 8 mm in diameter, of annealed chrome-vanadium and manganese steel, with transverse holes 1, 2, and 3 mm in diameter, the bars having an ultimate strength of about 100 kg/mm². Shafts of this type are are used, for instance, as driving and transmission shafts in engines. The results are summarized in Table I and are also shown in Fig. 5.

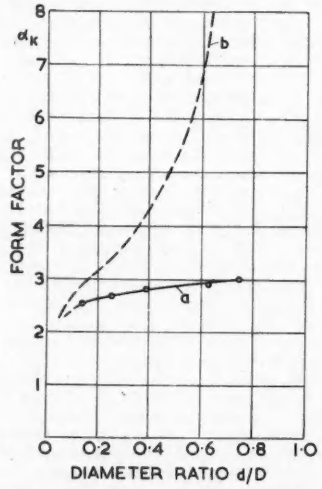

Fig. 3. **Form factor $\alpha_K = \tau_{max}/\tau_{nh}$ (curve *a*, referred to the hollow section), and $\alpha_K' = \tau_{max}/\tau_{ns}$ (curve *b*, referred to the solid section.**

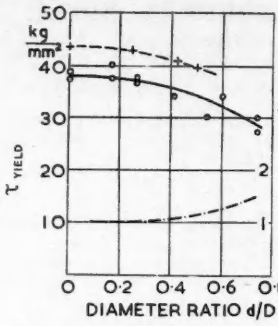

Fig. 4 (left). **Yield stress τ_{yield} of steel shafts as a function of the ratio d/D.**

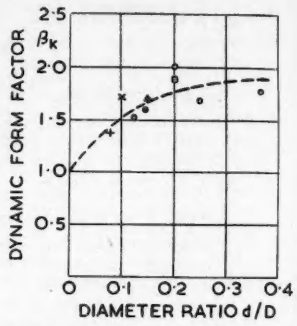

Fig. 5 (right). **Dynamic form factor $\beta_K = \tau_{dyn.\ solid}/\tau_{dyn.\ hollow}$ as a function of the diameter ratio d/D, in the case of alternating torsional stresses.**

\+ D = 40 mm U.T.S. = 85 kg/cm²
O D = 30 mm U.T.S. = 80 kg/cm²

TABLE I. TORSIONAL STRENGTH TESTS ON TRANSVERSELY BORED SHAFTS

Material	Ult. tensile strength kg/mm²	Shaft dia. D mm	Hole dia. d mm	Fatigue strength kg/mm²	Dynamic form factor β_K	Tests made by
Cr–V steel	100	8	0	32	1	Seeger
	,,	,,	1	20·5	1·55	O
	,,	,,	2	19	1·7	
	,,	,,	3	17·5	1·8	
V–Mn steel	100	8	0	30	1	Seeger
	,,	,,	2	17·5	1·7	O
Cr–Ni steel	100	30	0	23	1	Cornelius & Bollenrath
	,,	,,	2·5	16	1·4	+
,,	100	10	0	33	1	Dolan
	,,	,,	1	19	1·7	×
,,	100	14	0	25	1	Houdremont
	,,	,,	2	16	1·6	●
,,	95	10	0	29·5	1	Armbruster
,,	,,	,,	1·5	17·8	1·7	▽
,,	100	30	0	27	1	Lehr
,,	,,	,,	6	14	1·9	+
,,	100	15	0	30	1	Herold
,,	,,	,,	3	15	2	—O—

4. SUMMARY OF RESULTS

The tests confirmed the fact that in shafts subjected to torsional loading the maximum stresses occur in the vicinity of the edge of the hole. The stress peaks are situated on the 45 deg. tangents to the hole relative to the shaft axis, in the case of small hole diameters; and with increasing hole diameters the peaks shift towards the 90 deg. positions, i.e. towards the smallest effective cross-section. For static loads the form factor $\alpha_K = \tau_{max}/\tau_{nh} \simeq 2{\cdot}7$ should be used, while for dynamic loads the form factor is $\beta_K = \tau_{ns}/\tau_{nh} \simeq 1{\cdot}7$. The effect of the transverse hole on the yield strength is appreciable only when $d/D > 0{\cdot}3$.

The designer can, therefore, work on the basis of the following rules:—In cases of static or tensile stress, the nominal permissible stress should be reduced to 75 per cent, and for alternating stresses to 50 per cent of its original value. In cases of combined dynamic torsional and bending loads, the permissible stresses should be reduced to even lower values (according to Thum and Kirmser to 35 per cent of the permissible stress for the solid section).

To determine the nominal stress τ_{nh}, the section modulus of the critical section of the shaft with a trans-

verse hole can be calculated by means of the simple formula

$$Z_{\text{hollow}} = \left(1 \pm 0{\cdot}9\,\frac{d}{D}\right)\frac{\pi D^3}{16}$$

in all cases for which $d/D < 0{\cdot}5$. The maximum stress is then $\tau_{max} = \alpha_K\,\tau_{nh}$ or $\tau_{max} = \beta_K\,\tau_{nh}$ with the values for α_K and β_K indicated above.

BIBLIOGRAPHY

(1) THUM and W. KIRMSER: Superimposed alternating stresses. *VDI. Forschungsheft*, No. 419, 1943.

(2) NEUBER: *Kerbspannungslehre* (Stresses in perforated bars and plates.) Springer, Berlin, 1937.

(3) E. LEHR: Stress distribution in structural elements. *VDI Verlag*, 1934.

(4) L. FÖPPL: *ZVDI*, Vol. 65, 1921, p. 497.

RUSSIA

Gearless Drive for Tractors

By V. A. SVETOZAROV. (From *Vestnik Machinostroyenia*, No. 1, 1948, pp. 17-22, 6 illustrations.)

PRESENT-DAY agricultural tractors all suffer from one defect in design, namely, their gearbox drive, which does not permit of utilizing the power output which can be produced by the engine. The adoption of multi-speed drives does not solve the problem satisfactorily, as the required power at the tractor drawbar may change rapidly due to changes in terrain or acceleration of the combined unit, i.e., the tractor and attached agricultural machines. In view of this, the engine must be rated so as to be capable of supplying the momentary peaks of power demand. Therefore, the engine does not work at its economical rating, and as the sudden peaks cannot be foreseen, even the higher-rated engines may often stall—a very undesirable feature.

The fuel consumption of tractors is higher than is necessary, firstly, because the engine does not operate at the economical point, and secondly, under these conditions, the fuel consumption expended for the tractor itself becomes higher in relation to the useful work done than if the tractor were fully loaded.

The only solution to the problem is the adoption of a gearless drive, where the transmission ratio can be varied under load and when the tractor is in motion. This also permits the use of automatic speed adjustment corresponding to the changes in hauling effort.

The friction drive described in this article permits a smooth regulation of speed under all load conditions and considerably facilitates the handling of the tractor, thus permitting the driver to concentrate his attention on the agricultural machine served by the tractor. These features are particularly valuable for horticultural work.

The gearless drive is conducive to longer life for many parts of the tractor and agricultural machinery due to smooth starting and speed variation.

It was calculated that due to the inherent shortcomings of the gear drive, one thousand tons of fuel are wasted in Russia every day. Even more serious is the loss in tractor output, which could be raised by one-third if a more satisfactory type of transmission was introduced.

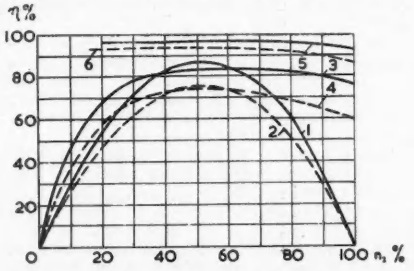

Fig. 1. **Comparison of efficiencies for various types of gearless drives.**

(1) Hydraulic drive for high power; (2) hydraulic drive for 45-hp engine; (3) hydraulic piston drive for high power; (4) hydraulic piston drive for engines of 30 to 45 hp; (6) friction drive, type C; (6) friction drive, type T.

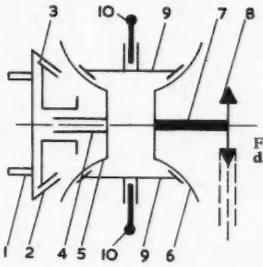

Fig. 2. **Diagram of friction drive for a Diesel-powered trolley.**

Electric drives are found to be too expensive, heavy and complicated. Moreover, their efficiency does not reach 0·8, so that any gains achieved as a result of smooth speed regulation are lost because of the low efficiency of the transmission.

Hydraulic drives are of smaller dimensions and suitable for service in tractors, but their efficiency is even lower than that of electric transmission.

The author has developed a mechanical gearless transmission which he calls the "friction drive" and which has been found entirely suitable for tractors; it is of compact design, can withstand sudden changes in load and has an efficiency which in many cases exceeds that of geared drives.

Two types of friction drive gear are being produced, the cheaper version, type T, having friction surfaces of cast steel and textolite, and type C with hardened steel surfaces having a higher efficiency. Fig. 1 makes it evident that the friction drive efficiency is very high and is not affected by speed variations.

Although it was decided to go ahead with large-scale production of friction drives for tractors, the War interrupted development, and the only practical

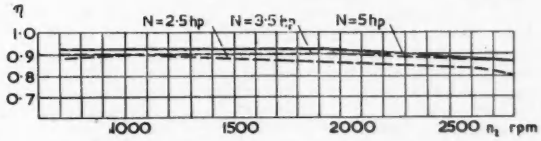

Fig. 3. **Efficiency (η) of transmission on the Diesel-powered trolley over the output rpm with varying power output and constant engine speed of 1450 rpm.**

experience that has been gained so far is in Diesel-driven trolleys for railway platform work. The engines employed were adapted stationary 5-8 hp Diesels of 1500-2000 rpm with a reduced size of flywheel. The latter fact, of course, renders the operating conditions more onerous. Type T friction drive was installed as shown diagrammatically in Fig. 2. The pins (1) engage with the engine flywheel and, through wheel

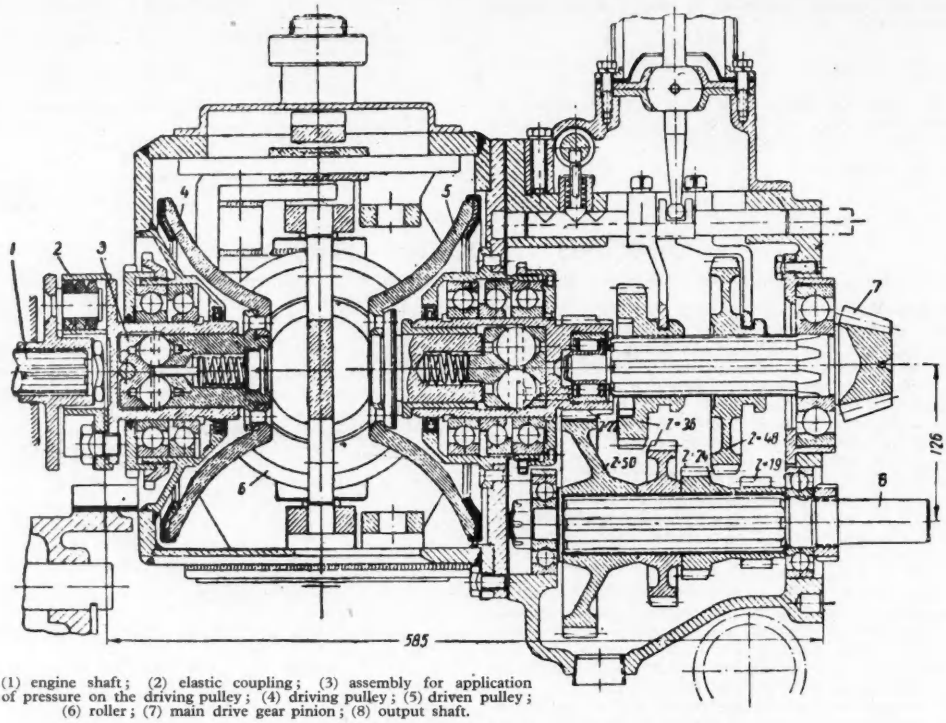

(1) engine shaft; (2) elastic coupling; (3) assembly for application of pressure on the driving pulley; (4) driving pulley; (5) driven pulley; (6) roller; (7) main drive gear pinion; (8) output shaft.

Fig. 4. **Friction drive for tractor.**

(3), drive the axle (4) to which is attached the shaped pulley (5). A second, identical, pulley (6) is mounted opposite (5) and is connected through a spindle (7) to the sprockets (8) which drive the wheels by means of a chain drive. The motion is transmitted between the pulleys (5) and (6) by two rollers (9). The transmission ratio is varied by revolving the rollers (9) around the pivots (10). The latter extend to the respective centres of the half-circles formed by the two pulleys (5) and (6). The pulleys are pressed against the rollers with a force which is proportional to the transmitted moment. The design of this automatic device is obvious from Fig. 4.

The friction drive is controlled by a single handle. When this is turned horizontally, the speed of drive is varied; when it is pressed up or down the coupling is engaged or disengaged respectively.

In spite of very unfavourable conditions for the design, due to space limitations, the efficiency of the friction drive in this case was 0·915 at rated power.

Fig. 3 gives the efficiency of transmission for varying output and speed, obtained on the test bench.

The trolley fitted with the friction drive has been in continuous service for a considerable time and has given every satisfaction under most unfavorable conditions. The weight of the trolley when empty is 900 kg and when fully loaded 2400 kg.

The friction drive installed in the type KD35 tractor (Fig. 4) gives a range of smooth speed variation which is adequate for agricultural uses. The gearbox shown in Fig. 4, in conjunction with the variable friction drive, gives the tractor an even wider range of speeds. Three separate ranges of stepless regulation are obtained with an engine speed of 1400 rpm:

(1) 3 to 11·9 mph for transport purposes.
(2) 1·3 to 5·2 mph for agricultural work.
(3) 0·6 to 2·5 mph for special and horticultural work.

If the engine speed is reduced to 800 rpm the tractor speed can be as low as 0·36 mph.

The transmission for tractors not required for such universal use can be made considerably simpler than that shown in Fig. 4.

The gearbox on the right of Fig. 4 can be simplified and used only for reversing the tractor, or it can be omitted altogether, for a design of friction drive is available which is suitable for reversing.

It is thought that the application of the friction drive will lead to the use of Diesel engines even on the smallest tractors, where previously petrol engines have been in common use. The higher weight of Diesel engines is not a deciding factor and the application of the friction drive will permit the use of smaller Diesel engines for the same hauling power, thus reducing the weight.

The smaller capacity of Diesels for overload without stalling, as compared with petrol engines, the former being 10-15 per cent as against 20 per cent in the latter case, becomes less important because overloading should not occur with a friction drive, particularly when automatic control is used.

The " Universal " tractor at present equipped with a 20-hp petrol engine would only require a 12 to 14-hp Diesel if a friction drive were used. Thus, the engine weight would remain as before and the fuel consumption would be halved, while its value would be reduced to an even larger extent. Similar considerations with regard to a friction drive would apply to other types of mobile agricultural machinery. It has been decided to go ahead with at least two types of tractors with a friction drive, one type having a single unit and the second type having two units for the individual control of each caterpillar.

Stresses in Locomotive Piston Rods with Unsymmetrical Crossheads

By F. ANGERER. (From *Maschinenbau und Wärmewirtschaft*, Vol. 3, No. 7, July, 1948, pp. 101-105, 4 illustrations.)

HEAVY express locomotives of the Austrian State Railways, after a few years running, experienced frequent piston rod failure which, in some cases, caused serious cylinder damage. The piston rods fractured at section *Z–Z* (Fig. 1) where the tapered shaft end (shown in Fig. 2) emerges from the crosshead. Cracks started at the uppermost surface of the shaft and spread downwards, and from the appearance of the fracture, it could be assumed that an alternating bending moment M_0 (Fig. 1) caused fatigue fracture of the shaft. This bending moment is due to acceleration forces acting on the crosshead, the centre of gravity of which has an eccentric position, with respect to the piston rod axis[1]. M_0 can be reduced by increasing the length of the crosshead guide and the following calculations show that such a limitation of M_0 is important.

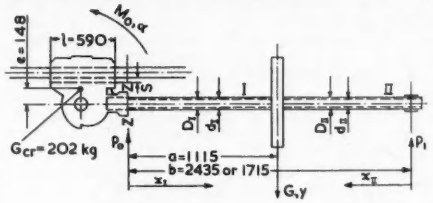

Fig. 1.

The original piston rods which failed had an outside diameter of $D_1 = D_2 = 98$ mm (3·86 in) and an inside bore of $d_1 = 55$ mm (2·17 in) and $d_2 = 80$ mm. (Dimensions refer to Fig. 1). Replacement piston rods were solid over length I, and finally the outside diameter was increased to 103 mm. The weight of the crosshead was 202 kg $= G_{cr}$ (446 lb) and its centre of gravity was found after measurement to be $e = 148$ mm (5·83 in) above the piston rod axis. The weight of the piston rod was 100 kg, and that of the piston, plus the rings 144 kg, giving a total weight of $G_p = 244$ kg (538 lbs). At the inner dead centre (I.D.C.), the steam pressure on the piston produces tension, and the inertia of piston and rod compression in section *Z–Z*. Under the influence of the outward acceleration of the piston, the inertia force exerted by the eccentric crosshead superimposes a bending moment M_0 in the direction shown in Fig. 1, so that a maximum tensile stress will arise in the upper extreme fibre of the shaft at

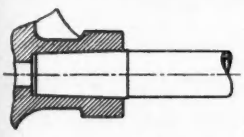

Fig. 2.

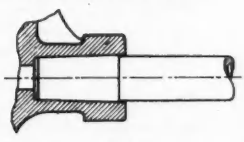

Fig. 3.

cross-section *Z–Z*. The maximum value of M_0 is determined by the maximum angle α through which the piston rod end can be bent:

$$\sin \alpha \triangleq \alpha = s/l,$$

where s = play between crosshead and slide and l = length of crosshead guide. At the outer dead centre (O.D.C.) all the forces are reversed so that the upper extreme fibre now carries a maximum compressive stress.

Let the piston shaft be supported by P_0 and P_1 (Fig. 1) and loaded by M_0 and G, where G = weight of piston plus half that of the piston shaft, i.e., about 190 kg. Then:

$$\left.\begin{aligned} G &= P_0 + P_1 \\ M_0 &+ P_1 b - G a = 0 \end{aligned}\right\} \quad (1)$$

Also, strain energy due to bending:

$$U = \int \frac{M^2}{2E_1}\,dx = U_1 + U_2$$

$$= \frac{1}{2EI_1}\int_0^a M_1^2\,dx_1 + \frac{1}{2EI_2}\int_0^{b-a} M_2^2\,dx_2 \quad (2)$$

where: $M_1 = M_0 - P_0 x_1$ and $M_2 = P_1 x_2$.

Integrating and introducing limiting values:

$$U = \frac{1}{2EI_1}\left(M_0^2\,a - M_0 P_0 a^2 + P_0^2\,\frac{a^3}{3}\right) + \frac{1}{2EI_2}\,P_1^2\,\frac{(b-a)^3}{3}$$

and substituting for P_0 and P_1 from eq. (1):

$$U = \frac{1}{2EI_1}(M_0^2\,k_{11} + M_0\,G\,k_{12} + G^2\,k_{13}) + \frac{1}{2EI_2}(M_0^2\,K_{21} + M_0\,G\,k_{22} + G^2\,k_{23}) \quad .. \quad (3)$$

where

$$k_{11} = \frac{a^3 - 3a^2 b + 3ab^2}{3b^2} \qquad k_{21} = \frac{(b-a)^3}{3b^2}$$

$$k_{12} = \frac{-3a^2 b^2 + 5a^3 b - 2a^4}{3b^2} \qquad k_{22} = \frac{-2a(b-a)^3}{3b^2}$$

$$k_{13} = \frac{a^3(b-a)^2}{3b^2} \qquad k_{23} = \frac{a^2(b-a)^3}{3b^2}$$

Finally, according to Castigliano's first theorem:

$$\alpha = \frac{\partial U}{\partial M_0} = \frac{1}{2EI_1}(2M_0 k_{11} + G k_{12}) + \frac{1}{2EI_2}(2M_0 k_{21} + G k_{22}) \quad .. \quad (4)$$

α is determined by the guide length of the crosshead (l = 590 mm = 23·3 in) and the play between crosshead and slide. A maximum play of 0·06 in has been allowed, but in the following calculation it is assumed that this increases through wear to a maximum of 0·08 in, so that $\alpha = s/e = 0{\cdot}0034$. The maximum bending moment M_0 can thus be calculated. According to Castigliano it is also:—

$$y = \frac{\partial U}{\partial G} = \frac{1}{2EI_1}(M_0 k_{12} + 2G k_{13}) + \frac{1}{2EI_2}(M_0 k_{22} + 2G k_{23}) \quad .. \quad (5)$$

where y, the deflection of the piston, shows whether the piston can impinge on, and perhaps damage, the cylinder walls. y_0, calculated from eq. (5) for the standstill of the locomotive ($M_0 = 0$), gives a measure

of the natural frequency of oscillation of the piston rod[2]:

$$f_n = \frac{300}{\sqrt{y_0}} \quad .. \quad .. \quad .. \quad (6)$$

where y_0 is in centimetres. All these values are given in Table I for the original dimensions of the piston shaft and for the shaft, assuming that the outside diameter has worn down to 93 mm. E has the usual value for steel.

TABLE I.

		I.D.C.		O.D.C.		I.D.C.
		(a)	(b)	(a)	(b)	(c)
$D_1 =$	D_2 mm	98	93			103
	d_1 mm	55	55			0
	d_2 mm	80	80			76
	I_1 cm^4	407·3	322·3	as for I.D.C.		552·5
	I_2 cm^4	251·7	166·1			388·7
	A_1 cm^2	51·7	44·2			81·7
	a mm	1115		1115		
	b mm	2435		1715		
	k_{11} cm	68		55·5		
	k_{12} cm^2	— 4740		— 2500		
	k_{13} cm^3	136000		564000		
	k_{21} cm	13		2·46		
	k_{22} cm^2	— 2900		— 550		
	k_{23} cm^3	162000		30500		
$\alpha =$	s/l	0·0034		0·0034		
	G kg	190		190		
	M_0 kg cm	44300	36400	—46200	—34500	57500
	y mm	—1·49	—1·455	1·01	1·04	—1·528
	y inches	—0·059	—0·057	0·040	0·041	—0·060
	y_0 mm	0·842	1·210	0·130	0·167	0·572
	f_n sec^{-1}	1035	862	2630	2330	1260

Negative deflections y are directed upwards.

Let the connecting-rod length be L = 4250 mm = 14 ft, the crank radius r = 360 mm = 14·2 in, the driving wheel diameter D = 1900 mm = 6 ft 3 in, and the train speed V in km per hour, then:—

$$\text{crank velocity } v = \frac{V}{3{\cdot}6} \times \frac{2r}{D} = 0{\cdot}105\ V \text{ [m/sec]}$$

$$\text{piston acceleration } a = \frac{v^2}{r}\left(\pm 1 - \frac{r}{L}\right) \text{ [m/sec}^2\text{]}$$

$$\text{bending moment } M_0 = \frac{G_{cr}}{g} \times a \times e = \frac{G_{cr}}{g} \times e \times \left(\pm 1 - \frac{r}{L}\right) \times \frac{(\cdot 105\ V)^2}{r} \quad .. \quad .. \quad (7)$$

and for e = 148 mm (Fig. 1),

$$M_0 = + 0{\cdot}106\ V^2 \text{ (kgm) (for I.D.C.).}$$
$$= - 0{\cdot}121\ V^2 \text{ (for O.D.C.).}$$

Since M_0 is already determined by the value of angle α, the minimum train speed at which M_0 will be reached can be calculated from this equation. The direct stress on the dangerous cross-section Z–Z of the piston shaft, due to inertia forces exerted by piston and piston rod, is

$$\sigma_p = \frac{Q_p}{A_1} = \frac{G_p}{g\,A_1} \times (-a) = \frac{G_p}{g\,A_1} \times \left(\mp 1 + \frac{r}{L}\right) \times \frac{(0{\cdot}105\ V)^2}{r} \quad (8)$$

i.e.,

$$\sigma_p = \frac{-0{\cdot}697\ V^2}{A_1} \text{ (kg/cm}^2\text{) for I.D.C., } \sigma_p = \frac{+0{\cdot}786\ V^2}{A_1}$$

(kg/cm^2) for O.D.C.

If the piston diameter D_p = 650 mm = 25·6 in and the maximum steam pressure in the cylinder p = 14 atm = 206 psi, then the direct stress on Z–Z due to steam pressure on piston is:

$$\sigma_{st} = \frac{Q_{st}}{A_1} = (65^2 - 10^2)\frac{\pi}{4} \times \frac{14}{A_1} = \frac{45500}{A_1} \text{ [kg/cm}^2\text{]} \quad (9)$$

The bending stress on Z–Z, due to M_0, is

$$\sigma_b = \frac{M_0}{I_1} \times \frac{D_1}{2} \text{ [kg/cm}^2\text{]} \quad .. \quad .. \quad (10)$$

and, finally, the resultant maximum fibre stress in the uppermost fibre of the piston rod at section Z–Z is:

$$\sigma_{max} = \sigma_p + \sigma_{st} + \sigma_b \quad .. \quad .. \quad .. \quad (11)$$

Numerical values of these stresses are given in Table II, tensile stresses being assumed as positive, and compressive stresses as negative.

CONCLUSIONS

The natural frequency of vibration of the rod is so high that resonance phenomena cannot have been a cause of the piston rod failure. The train speed V at which the maximum bending moment M_0 is just reached is also the critical speed at which the resultant stress in the piston rod is highest. The inertia force of the piston has to be deducted from the steam force, and since this inertia force increases with V^2, the resultant stress decreases as the train speed increases above the critical value. The bending stress increases appreciably as the play between the crosshead and crosshead slide is increased. Comparison of numerical stresses given in Table II with those calculated for the heavier piston rod sections used to replace the failing piston rods shows that, at the critical speed, bending and inertia stresses do not vary appreciably, but the direct stress exerted by the steam pressure on the heavier cross-section is decisively reduced. The critical speed increases slightly for heavier shaft sections and increasing crosshead play, but in all cases remains within 30 to 46 miles per hour.

TABLE II.

	I.D.C.		O.D.C.		I.D.C.
	(a)	(b)	(a)	(b)	(c)
M_0 kg cm	44300	36400	—46200	—34500	57500
V_{cr} km/hr	64·7	58·6	68·0	53·2	73·7
V_{cr} mph	40·2	36·4	42·6	33·0	45·7
σ_p kg/cm^2	—56	—54	70	50	—46
σ_{st} ,,	861	1008	—861	—1008	545
σ_b ,,	534	525	—556	—487	528
σ_{max} ,,	1339	1479	—1325	—1445	1027
σ_{max} psi	19000	21000	—18800	—20600	14600

Positive stresses are tensile, negative stresses compressive.

The maximum resultant stresses are very high. If stresses due to the tapered fit are added to these stresses, and if, furthermore, the danger of a notch effect at section Z–Z is added and a concentration factor of 3 allowed, the total stresses can easily exceed the fatique strength (18 tsi) of the steel used (38-ton steel). A notch may be caused mechanically by the dynamic moment (— M_0) acting on the crosshead in O.D.C. position, or chemically by corrosion. This danger, however, can be eliminated if design Fig. 3 is chosen instead of Fig. 2, i.e. if the piston rod taper is made to finish *inside* the tapered recess in the crosshead. The improved design has already been successfully applied to the hubs of wagon wheels.

BIBLIOGRAPHY

(1) GARBE, Modern steam locomotive, 2nd edition, p. 331.
(2) HÜTTE, 25th edition, Vol. 1, p. 404.

DESIGN AND WORKSHOP

A Digest of articles of interest to Works Managers, Planning and Production Engineers, Superintendents, Jig and Tool Designers, Inspectors, Time Study Engineers, and all those concerned with the practical aspects of Engineering.

Control of Carbon Content during Heat Treatment of Steel in Atmosphere Furnaces

By W. H. HOLCROFT and E. C. BAYER. (From *Materials & Methods, U.S.A.*, Vol. 28, No. 2, August, 1948, pp. 59-61, 6 illustrations.)

FURNACE atmospheres are composed of a diluent or carrier gas to which is added a hydrocarbon gas in the amount required by the particular heat treatment process. The most common carrier gas used today is the catalytic generator gas produced by the pyrolysis of a controlled air-gas mixture in an externally-heated retort in the presence of a suitable catalyst. A typical analysis of a catalytic generator gas using natural gas in the cracking reaction is: 0·1 to 0·3 carbon dioxide, 20·0 carbon monoxide, 0·6 methane, 40·0 hydrogen, 0·22 to 0·35 per cent water vapour (dewpoint +10 to +20° F), balance nitrogen.

For every furnace temperature, the equilibrium conditions of the furnace atmosphere will vary. These conditions are determined by the following reactions:

$$2\,CO \rightleftarrows CO_2 + C$$

$$K = \frac{(CO)^2}{(CO_2)} \quad \ldots \quad (1)$$

$$H_2O + CO \rightleftarrows H_2 + CO_2$$

$$K = \frac{(CO) \times (H_2O)}{(H_2) \times (CO_2)} \quad \ldots \quad (2)$$

In each reaction the equilibrium constant, K, increases with increasing temperature.

In Figs. 1 to 4 are plotted the carbon dioxide percentage versus the partial pressures of the carbon monoxide and carbon dioxide content which are in equilibrium with a given carbon content of the steel at various temperatures. The carbon dioxide content referred to is the actual percentage of carbon dioxide gas in the furnace atmosphere as determined by standard gas analysis. The partial pressure, in atmospheres, is the pressure exerted by the combined carbon monoxide and carbon monoxide and carbon dioxide content as determined by the same gas analysis—i.e, the sum of the percentages of these two gases.

For each temperature, the carbon activity of saturated austenite is taken as unity (100 per cent). For lower carbon concentrations, the carbon activity decreases as a straight-line function. Thus, if at 1500° F steel of 1·00 per cent carbon (saturated austenite) has a carbon activity of 1, then 0·60 per cent carbon steel will have a carbon activity of $\frac{0{\cdot}60}{1{\cdot}00} \times 1$, or 0·6; and K for equilibrium with 0·60 per cent carbon steel at 1500° F would then be 8·15 × 0·6, or 4·89, where 8·15 is the constant, K, for saturated austenite at the same temperature.

HOW TO USE THE CURVES

The accompanying curves showing the carbon monoxide-carbon dioxide equilibrium conditions are sufficiently complete for practical application to most carbon-control atmosphere conditions encountered in industry today. To determine the carburizing potential of a furnace atmosphere, it is only necessary to analyze the atmosphere for carbon monoxide and carbon dioxide content and refer to the appropriate graph. For example, assume that a carburizing furnace is operating at 1600° F and that the furnace atmosphere analyses 0·15 per cent carbon dioxide and 14·85 per cent carbon monoxide. The partial pressure in this case would be 0·0015 plus 0·1485, or 0·15 atmospheres. Referring to the 1600° F curve (Fig. 2), for a partial pressure of 0·15 atmospheres and a carbon dioxide content of 0·15 per cent, as shown at point A, we find the equilibrium content of the steel to be 0·80 per cent carbon. This means that with the furnace conditions stated above, the surface carbon content of the steel would not be higher than 0·80 per cent carbon.

Likewise, an atmosphere containing 0·6 per cent carbon dioxide and 24·4 per cent carbon monoxide at 1600° F would have a partial pressure of 0·25 atmospheres. This condition is represented by point B (Fig. 2); and the graph indicates that this atmosphere is decarburizing to a 0·60 per cent carbon steel, carburizing to a 0·40 per cent carbon steel, and in equilibrium with a steel of about 0·55 per cent carbon. Point C, Fig. 2 indicates a condition where carbon dioxide content is 0·4 per cent carbon steel, carburizing to a 0·20 per cent carbon steel and in equilibrium with a steel of approximately 0·30 per cent carbon. A completely decarburizing condition is represented by point D, where the furnace atmosphere analyses 0·4 per cent carbon dioxide and 9·6 per cent carbon monoxide, with a resulting partial pressure of 0·10 atmospheres.

These curves clearly show that for a hypereutectoid case, the carbon dioxide content of the furnace atmosphere must be very low, whereas the lower surface carbon concentrations do not require an atmosphere devoid of carbon dioxide. For a given surface carbon concentration, the carbon dioxide content allowable in the furnace atmosphere is greater at lower temperatures.

It is also true that inter-gas reactions give a higher carbon dioxide content at lower temperatures. For example, consider a sealed chamber containing a gas atmosphere and some solid carbon. If the chamber is heated to 1700° F and held at that temperature, a state of equilibrium will be established between the solid carbon and carbon dioxide and monoxide gases ; for the solid carbon will react with the carbon dioxide to form carbon monoxide until equilibrium is reached, according to reaction (1). If the temperature is dropped to 1500° F and sufficient time allowed, some of the carbon monoxide will break down into carbon and carbon dioxide until a new equilibrium condition is reached.

Under practical furnace conditions, for an atmosphere containing 20 per cent carbon monoxide, 40 per cent hydrogen and the balance nitrogen at 1700° F, the equilibrium analysis would be 0·08 carbon dioxide, 20·0 carbon monoxide, 40 hydrogen, 0·22 per cent water vapour (a dewpoint of plus 10° F) and balance nitrogen, in accordance with equation (2). At a reduced temperature of 1500° F with 20 per cent carbon

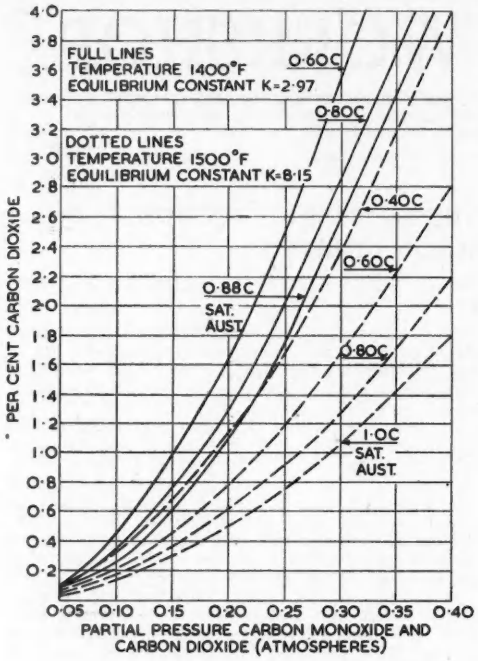

Fig. 1.

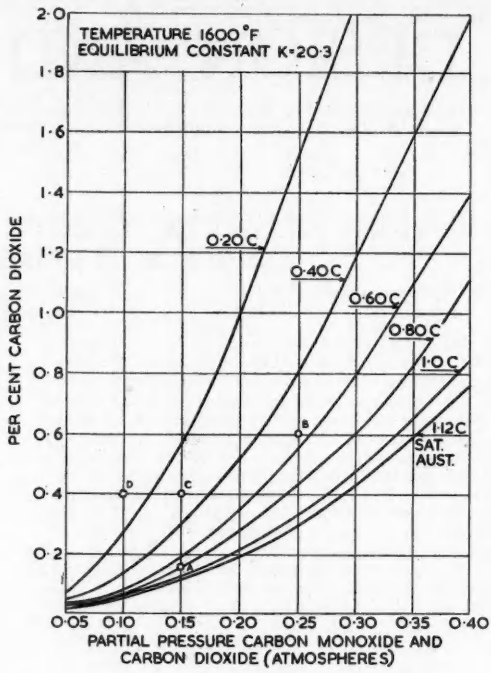

Fig. 2.

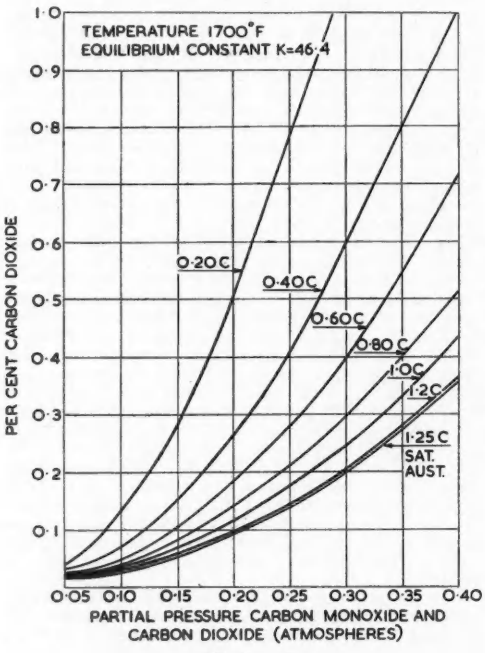

Fig. 3.

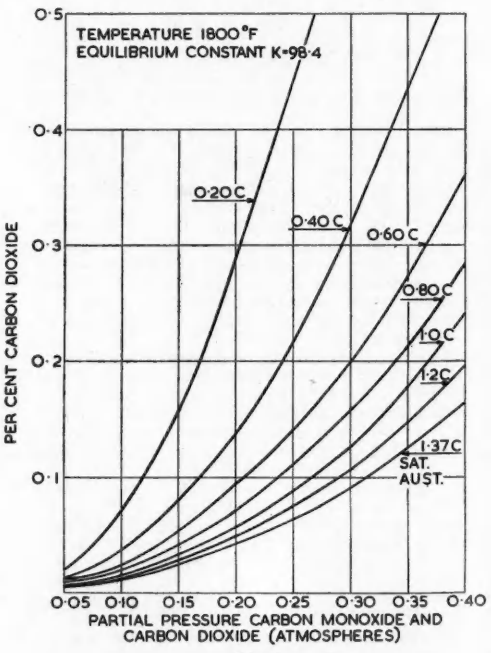

Fig. 4.

monoxide, the resulting equilibrium values for carbon dioxide and water vapour would be 0·48 and 0·9 per cent, respectively.

It should be noted that a difference in hydrogen content will result in a variation in the dewpoint. For two atmospheres of equal carburizing strength, the one

having the higher hydrogen content will have the higher dewpoint, as indicated by equation (2). Therefore, a dewpoint determination must be carefully considered in relation to the hydrogen content when evaluating the carburizing strength of an atmosphere.

In gas carburizing at about 1700° F, the hydrocarbon addition will react with the carbon dioxide in the furnace atmosphere until equilibrium is reached. At lower temperatures, the hydrocarbon reaction will be slower, and consequently a carbon dioxide content higher than equilibrium with saturated austenite may be obtained even with excess hydrocarbon present. In any case, an accurate measurement of carbon monoxide and dioxide should indicate the equilibrium surface carbon content of the steel.

It should be remembered that the equilibrium curves represent conditions which are more nearly approached in carburizing than in hardening operations. For hardening, an atmosphere might be in equilibrium with say a 0·60 per cent carbon steel for a given temperature, but the amount of carbon added to a 0·40 per cent carbon steel, or removed from a 0·80 per cent carbon steel, would be negligible due to the time factor as well as to the small amount of carbon available before equilibrium would be reached.

Finally, it should also be remembered that equilibrium conditions are determined by the gas inside the furnace chamber and *not* by the gas *entering* the furnace. It is not necessary to introduce a zero-carbon dioxide generator gas into a furnace operating at 1500° F, as carbon dioxide will be formed in the furnace in accordance with equation (1).

The Development of the Gas Shielded Metal Arc Welding Process

By J. S. SOHN and A. N. KUGLER. (From a Paper delivered at the Annual Meeting of the *American Welding Society*, October 27, 1948.)

FOR many years it has been recognized that existing welding processes are not completely satisfactory for the joining of many metals. This deficiency is particularly apparent when welding relatively heavy sections in the vertical and overhead positions, and is accentuated when working with non-ferrous metals. In an effort to develop a better welding process, attention has been directed to the development of a method in which a consumable filler wire is continually deposited in a controlled gaseous atmosphere. The problems surrounding this new approach have been many, involving new concepts of a combination of factors including current density, gas shielding, and filler wire feed speeds. The results of this program have been most successful, culminating in the development of a new process known as the Aircomatic Process developed by Air Reduction Laboratories, Murray Hill, New Jersey. It may also be designated as gas shielded metal arc welding.

Briefly, this new process consists of feeding a bare or processed filler metal in wire form through a suitable holder. This filler metal carries welding current and an arc is maintained between the end of the wire and the work. Power may be supplied from a standard welding generator. The arc is maintained within a controlled envelope of shielding gas. The equipment developed for the process includes both a manual gun and automatic head.

With the manual unit, welding may be performed in all positions, i.e., flat, horizontal, vertical, and overhead. All of the standard joint designs may be welded in these positions. Single or multi-layer welds can be deposited using either beading or weaving techniques. Vertical welds may be made with either upward or downward travel.

The Aircomatic Process is particularly adapted to the welding of aluminium and its alloys. It has been found that direct current, reversed polarity, provides the necessary arc conditions. Standard d.c. welding generators, including constant potential multiple operator units, are suitable for this work. Argon has been found to be a satisfactory shielding gas for aluminium welding.

One of the principal features of this process is the use of very high current densities. Current densities twelve times those used in ordinary metal arc welding have been successfully employed. With such high current densities it becomes necessary to provide high rates of filler metal feed in order to make satisfactory welds. Filler wire speeds for the manual welding gun range from 100 to 300 inches per minute.

The arc obtained with this process may be described as a non-sensitive arc, since changes in arc length result in smaller changes in arc voltage than are encountered in normal metal arc welding. Observation of the arc discloses that it consists of a relatively narrow incandescent core surrounded by an umbrella shaped envelope. The outer envelope of the arc provides a cleaning action thus eliminating the need for welding fluxes.

For the manual welding of aluminium as currently provided in this process, only three sizes of filler metal are needed—viz. $^{3}/_{64}$ in, $^{1}/_{16}$ in, and $^{3}/_{32}$ in. With these filler metal sizes the overall current range is 70-450 amperes which permits welding of metal thicknesses from $^{1}/_{8}$ in up to 2 in and more.

The selection of filler metal composition is governed by the metal to be welded.

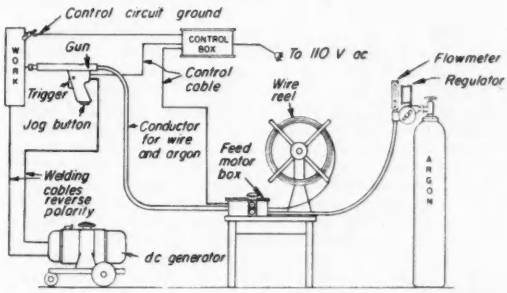

Fig. 1. **Schematic diagram of equipment for inert gas arc welding of aluminium.**

The component parts of the manual unit are illustrated schematically in Fig. 1. Starting with the welding gun it will be observed that it has (1) an attached welding cable from the generator ; (2) a gas (argon) hose, concentric with which is the metallic tube for conveying the filler metal wire ; and (3) a small, three conductor, control cable. The gas hose and wire conductor are connected, at the other end, to the feed motor box; the control cable also connects with this box. This feed motor box contains the governor controlled motor, speed reducer, feed rolls, and a solenoid valve. The control box, which is connected by the three conductor cable to both the gun and the feed motor box, contains the relays which control operation

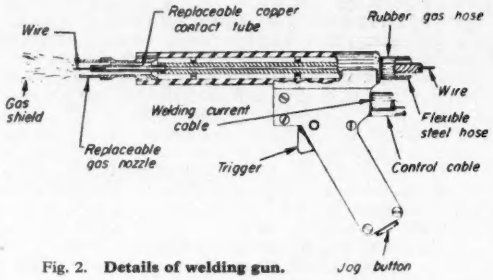

Fig. 2. **Details of welding gun.**

of the wire feed. The remaining piece of equipment is the wire reel for the filler metal.

The gun, shown diagrammatically in Fig. 2 is equipped with a trigger which readies the unit for welding and a "jog button" for feeding wire when not welding. To start welding the trigger is depresssed, and this starts the argon flow which purges the lines. Next the electrode, which should project $^1/_2$ to $^3/_4$ inch from the gas nozzle, is scratched on the work and when arc voltage is established, the controls operate to energize the feed motor and deliver filler metal. If desired, a current contactor may be placed in the welding circuit and connected through the control circuit to be operated by the trigger on the gun. When using a contactor the trigger is used for starting and stopping the welding. One of the advantages of using a contactor is that the gun is "dead," when the trigger is in the released position.

From Fig. 1 it will be noted that the gun is essentially simple, since most of the control and driving mechanisms have been placed in the other units. The argon passes down the "barrel" of the gun and issues from the gas nozzle around the wire electrode. Since both the gas nozzle and the wire guide tube are close to the welding arc they will gradually deteriorate and are, therefore, expendable items. In consequence these parts are of simple construction to permit of rapid and economical replacement.

The wire and the argon are carried in one conductor. The feed motor box contains the governor-controlled driving motor which provides the variable speeds necessary for the filler metal feed. This motor, operating on a 110 volt circuit, drives a pair of feed rolls through a speed reducer. The rolls draw the filler metal wire from the reel and propel it to the gun. This box also contains the solenoid valve which turns "on" and shuts "off" the flow of argon as controlled by the trigger on the gun. From the solenoid valve the gas is fed to the combination gas-wire feed conductor by means of a plastic hose and a tee connection.

The speed of wire feed is controlled by a manually set, mechanically governed motor. This speed, once established, remains constant regardless of what takes place at the welding arc. Selection of a welding current and a wire feed speed for a given size of filler wire results in a definite arc length and hence arc voltage. Thus, changes in arc length may be accomplished by either of the following methods (1) by varying the wire feed speed through the governor on the motor, or (2) by changing the current. In the first instance, assuming a given welding generator setting, increases in wire feed speed result in a decrease in arc voltage; obviously, such a decrease in arc voltage is accompanied by an increase in welding current, the value depending upon the characteristics of the d.c. generator used. It follows that decreases in wire feed speed have the opposite effect. In the second instance, assuming constant wire feed speed, changes in welding generator setting result in an increase in arc voltage when the machine setting is raised and a decrease when the setting is lowered. This inherent self-regulation of the arc resulting from the specific combination of a drooping generator characteristic and high burn off rate makes this welding process essentially automatic.

For welding aluminium it has been found that the flow of argon is not critical as long as it is maintained within reasonable limits. When welding with the manual gun, argon flows between 20 and 50 cu ft/hr are used. In general the lower flows are for low current values and the higher flows for the larger currents. Once the flow has been determined for a given welding condition it may be varied by as much as plus or minus 10 per cent without adversely affecting the welding operation. It has been demonstrated experimentally that up to 20 per cent more argon will be needed when welding fillet welds on tee joints, in order to provide shielding gas at the root of the joint.

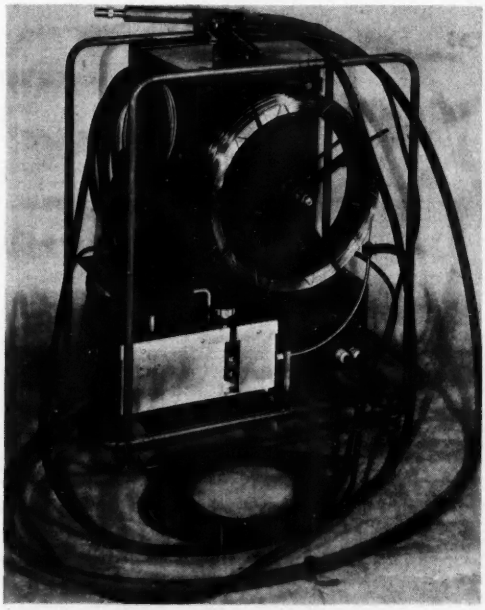

Fig. 3. **Welding equipment.**

Mechanical properties of aluminium welds are equal to the properties obtained in castings of the same analysis as the filler metal. The quality of welds produced in aluminium by this process is, as indicated earlier, dependent upon many variables. It may be stated generally that the welds will be superior to welds made with aluminium metal arc electrodes. Further, under proper conditions the quality will approach that obtainable with the inert gas-tungsten arc method. The welds are of excellent surface appearance. Porosity may be encountered in aluminium welds and is of two distinctive types: internal porosity readily visible with radiographic techniques and micro-porosity not detectable using normal radiographic procedures. The former is subject to control while the latter appears to be associated with most rapidly cooled cast aluminium alloys. In addition to the previously mentioned precautions, it is recommended that both aluminium base metal and filler metal be cleaned to ensure the production of high quality welds.

Attention is directed to the fact that welding of heavy aluminium sections may be accomplished with little or no preheat. This practice is in sharp contrast to other processes wherein the filler metal is added by indirect methods.

"Bandurko" Type Screw-Cutting Head for Pipes

By B. A. KURENKOV. (From *Stanki i Instrument, Russia,* No. 12, 1947, pp. 12-16, 11 illustrations.)

SCREW-CUTTING of pipes presents certain difficulties, due to their length and the required accuracy. To achieve the latter, the facing, turning and screw-cutting must be done in one operation. Similar requirements apply to nipples, although the thread is, of course, external.

To increase the speed of production, a screw-cutting head has been designed which meets all requirements and considerably simplifies the process; it can be used in the manufacturing industries as well as on repair sites.

The screw-cutting head is screwed onto the lathe spindle, while the pipe is held in a bracket resting on the support. Fig. 1 shows the design of the Bandurko head. Eight cutting dies (1) are fitted on the spindles (2), the latter having half of their circumference geared. The spindles engage with the internally toothed ring (3); when the ring (3) is turned, all eight spindles revolve and move the cutting dies into or out of the operating position. The ring (3) is under tension from the springs (4), which tend to turn it, and is fixed to a second ring (5), the recesses of which contain spring-loaded plungers (6). The body of the cutting head (7) has holes drilled in for the admission of oil to the cutting dies. As soon as the screw is cut, the pipe begins to press on the disk (8) revolving in the ball bearings (9), and moves the sleeve (10), which disengages the plungers (6) from the ring (5). This frees the geared ring (3), which is then turned by the force of the springs (4), withdrawing the cutting dies from their working position. To re-engage the cutting dies, it is necessary to turn the sleeve (10) by hand until the plungers drop into the recesses of ring (5).

The cone of the cutting head serves as a seat for the holders and cutting tools for the preparatory turning and facing of the pipe (Fig. 2). When the holder is attached to the head by means of the screw shown in Fig. 2, the latter presses on the piston (13), moving it to the right and

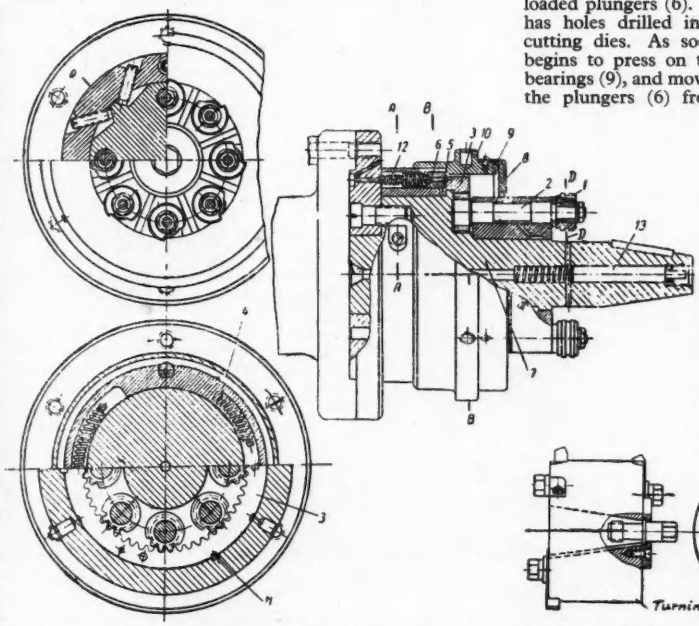

Fig. 1. **Bandurko type screw-cutting head for pipes.**

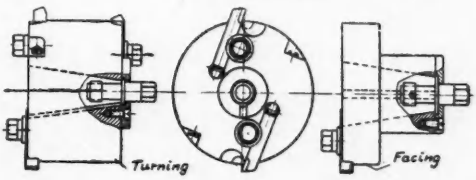

Fig. 2. **Tool-holding assembly for attachment to the cutting head for the purpose of turning and facing the pipe.**

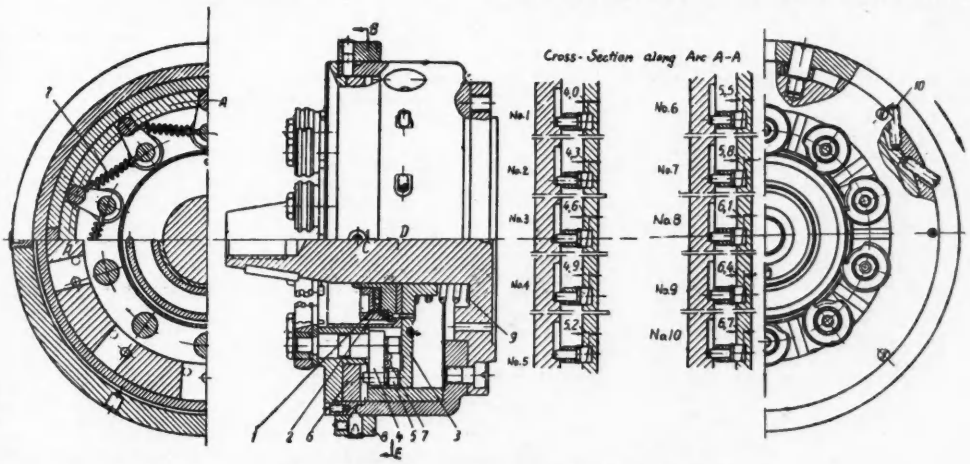

Fig. 3. **Bandurko type screw-cutting head for nipples.**

shutting off the oil supply to the screw-cutting dies.

Fig. 3 shows a cutting head designed on the same principle, but intended for cutting threads on nipples. The turning down and facing of the nipples is achieved by a cutting tool assembly similar to that shown in Fig. 2. The thread is cut in a single operation by means of ten cutting dies. To terminate the operation, the pipe presses on the ring (1), which, in turn, moves the disk (3) along the head. An important difference in design is that the cutting dies are disengaged progressively one after the other in order to obtain a smooth ending of the thread. The spindles (4), on which the cutting dies are fixed, carry dowels (5) which, at one end, engage in recesses in ring (3) and, at the other, engage in slots in ring (6). The ends protruding into ring (3) are of different lengths and, therefore, do not disengage simultaneously (see section along arc *A-A*). Immediately the dowel disengages, the spindle is turned by spring (7) and withdraws the cutting die from its working position. To load the head, sleeve (8) is turned by hand, carrying along the ring (6) and the dowels (5), thus revolving the spindles (4) until the other ends of the dowels drop into the recesses of disk (3), which is pushed to the left by the spring (9).

Accurate adjustment of the dies is achieved in both types of heads by means of screws (10).

Each size of pipe or nipple requires a separate head for the cutting of its thread, this being quite acceptable in a manufacturing shop, as large numbers of pipes or nipples can be cut in a batch and the changing of cutting heads takes very little time.

In certain cases, it is necessary to be able to deal with a whole range of pipe sizes, using one head only. Fig. 4 shows the design of a simplified universal head suitable for various sizes of pipes. The housing (1) is drilled eccentrically and a bush (2) is inserted. The holder (3) for the cutting tool is inserted in the bush and pressed against the cover (4). For small pipes, the cutting tool is fixed to the holder (3) direct; for medium pipe diameters, a second cutting tool assembly is fitted on the cone of (3), and for large diameters another assembly is screwed onto the flange (6). This flange is moved into its working position and out of this position by turning the eccentric bush (2), which, in turn, is operated by the ring (9) and the dog (10).

Fig. 5 shows the automatic device for disengaging the cutting head. When the required length of thread is cut, the support begins to push the rod (1) to the left, moving the pin upwards. The latter engages the plunger (11) in Fig. 4 and turns the ring (9) until the plunger drops into a recess in the flange (6). The bush (12) enters a recess in rings (9), permitting the spring (13) to move the slide block (14) forward, thus acting on the ratchet on the feed drum (8). The loading of the cutting head is achieved by means of the handle (3), Fig. 5. An eccentric connected to the handle moves a bush (4) upwards, which acts as a brake on ring (9) (Fig. 4). Ring (9) turns the bush (2) until the finger (7) rests on the drum (8). Screw-cutting with this head is done in several operations, and the automatic action as well as the simple manner in which the cutting head is mounted on a lathe make it a very valuable aid for cutting pipe-threads.

Attachments can be provided for the facing and turning of pipes previous to the screw-cutting, these attachments being similar to those described in the case of the Bandurko cutting heads used for a single pipe diameter.

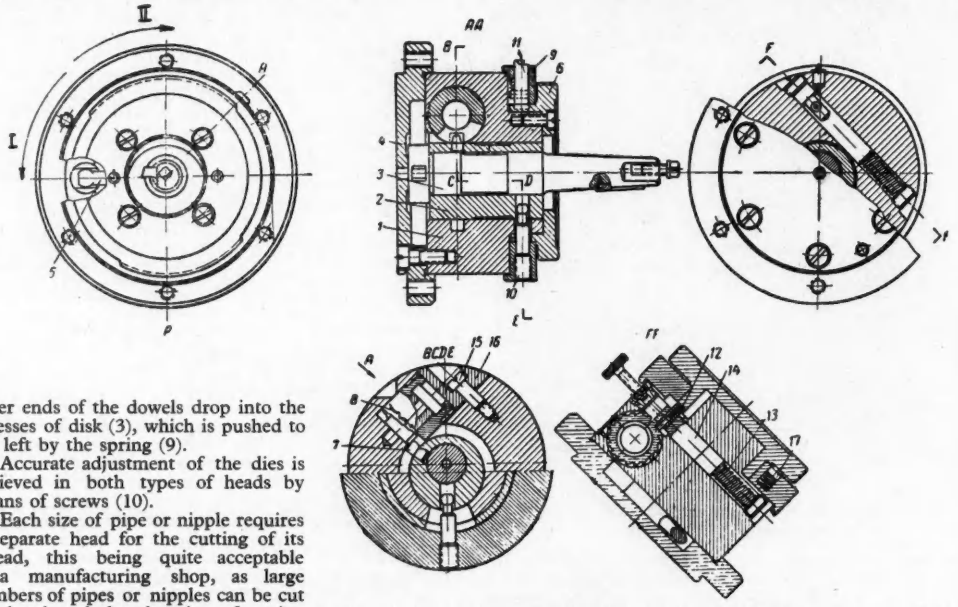

I = Normal direction of rotation. II = Direction of rotation when disengaging cutting die.

Fig. 4. Universal head for pipes and nipples.

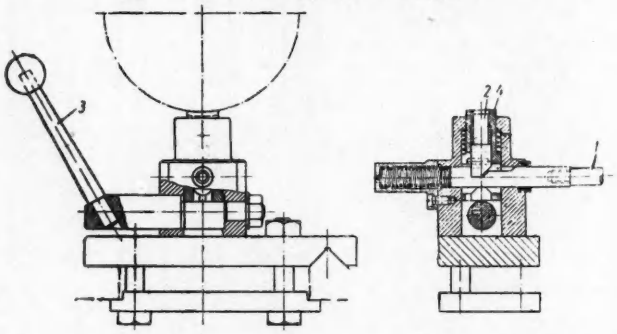

Fig. 5. Attachment for automatic disengagement and loading of universal screw-cutting head.

Bar Extension Tubes for Capstan Lathes and Automatics

By W. F. Troescher. (From *Werkstatt und Betrieb, Germany*, Vol. 81, No. 6, June, 1948, pp. 158-161, 8 illustrations.)

Bar materials must be fed into the hollow spindles of capstan lathes and automatics through long extension tubes which hold the bar, safeguard against accidents, permit automatic turning from very long bars, reduce noise and, by reducing or avoiding vibration, ensure smooth machined surfaces. The tubes can be designed as fixed or rotating tubes, with or without an internal elastic or shock-damping lining. Unlined fixed tubes are hardly used any more, except on machines for large bar diameters and slow cutting speeds and for turning exceptionally long cylindrical bars. Rotating tubes are supported on ball bearings and driven by positive drive or only friction, and rotate at the same speed as the bar material. The machine, therefore, runs more smoothly and with less noise. When fixed tubes are used, the running qualities can be improved by inserting fabric-base bakelite linings in the tubes. These damp the recurring shocks as the bar strikes against the tube wall. However, they are worn down very quickly and must be entirely replaced. Rotating tubes have also been designed to contain a damping lining of bakelite; wear is then considerably reduced. Finally, an elastic lining can be used, consisting of a close-wound helical spring extending over the entire tube length, with a sinusoidally varying mean coil diameter, so that the largest turns are pressed against the tube wall whilst the smallest turns hold the bar material elastically. The plastic linings must be adapted to the diameter of the bar material and linings of different thicknesses must be kept in stock, but even then a small clearance must be maintained between the bar and lining, so that the bar cannot be guided strictly centrally. Elastic linings automatically adjust themselves to a certain range of diameters and always guide the material centrally. That this is a real advantage is shown by the following considerations.

Let us first take the case of medium spindle speeds, e.g., up to 1500 rpm. If the bar has been well straightened, but slightly bent during transport, it will be deflected on rotation, if unsupported outside the hollow spindle, and will take the shape indicated by a thin line in Fig. 1. Disregarding the effect of the dead weight, the centrifugal force exerted by the bent end of the unsupported rotating bar is

$$Z = m\,r\left(\frac{2\pi n}{60}\right)^2 = \frac{\pi^2}{900g}\,Grn^2,$$

where G is the weight of the part which is deflected from the true axis, r the deflection, n the revolutions per min. The elastic material opposes further deflection by a restraining force

$$Z = r\,\frac{3\,EI}{a^3},$$

where I is the second moment of area, E the modulus of elasticity of the material, and a the unsupported length of the bar. Equating the two expressions we obtain

$$G = \frac{2700\,g}{\pi^2} \times \frac{EI}{n^2\,a^3}\;;\; G = \frac{C}{a^3}$$

for constant n.

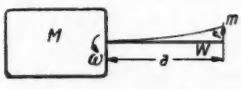

Fig. 1. **Schematic representation of machine tool M with rotating unsupported bar W.**

ω = angular speed, r = deflection of bar, m = eccentric mass, a = free length of bar.

This equation shows that G, the deflected weight, is independent of the deflection r but is proportional to E and I. n and a can only be increased if G is reduced, i.e., if the bar has been straightened more accurately at the start. Now, the spring lining will hold the bar over the whole tube length so that the free-length value a can be assumed to reach from the spindle end to the bar centre, whereas with a plastic lining there is play between the lining and bar and the value a is considerably greater and may even extend over the whole bar length. In this latter case, a would be doubled and G increased eightfold by the use of the plastics as compared with the spring lining. When using a spring lining, the bar material need not be straightened as accurately as is necessary when using the plastic lining. In the case of Fig. 2, with the tube and bar centrally guided at the end, and $b \doteq 2a$, we obtain the expression

$$G = 4{\cdot}6\,\frac{2700\,g}{\pi^2} \times \frac{EI}{n^2\,a^3} = \frac{C_1}{a^3}$$

This is fundamentally the same as in the case of Fig. 1, except that the eccentric weight G can now be 4·6 times greater if all other factors are the same as before.

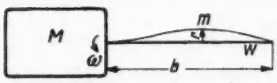

Fig. 2. **Schematic representation of machine tool M with rotating bar W supported at a distance b.**

ω = angular speed, r = deflection of bar, m = eccentric mass.

At speeds higher than about 1500 rpm, the whirling effect must be taken into account. The deflection does not increase simply with increasing turning speed, but shows a maximum value at the critical whirling speed which, according to experience, lies at about 1500 rpm. At this critical speed, the bar strikes violently against the tube, turns very irregularly and transmits vibrations to the extension tube and the machine frame. A clean turning process is then impossible. At speeds higher than the critical, the bar material again runs quietly, and clean turning is possible above as well as below the critical speed. This can be explained by reference to Fig. 3. Let the outer circle be the circumference of the deflected cross-section of the bar material, S its centre of gravity, O the point of intersection of the bearing centre axis with the deflected cross-section when at rest. $OS = e$ is then the deflection of the cross-section shown. At high rotational speeds, the bar tends to rotate about S and not about the bearing centre axis O. O tends to travel on the small circle shown in Fig. 3. This means that the cross-section shown is acted upon by the turning moment and, additionally, by a bending moment due to the eccentric travel of O. The material again exerts an elastic restraining force opposing the bending action, i.e., tending to force the bearing centre back to its original position O. Assume that O, during its travel, has reached point A_1. The restraining force then has the direction A_1O and its value is proportional to the distance A_1O. The case is similar for A_2 and A_3. Dividing this restraining force into its vertical and horizontal components, one can see that over one whole revolution the vertical components cancel out, but all the horizontal components are directed towards the left (Fig. 3) and thus add up. A mean value of the force restraining bending, therefore, exists and tends to displace the centre of gravity S constantly towards O (left in Fig. 3) since O is fixed in space. S is not pressed radially outward as it would be at low rotational speeds.

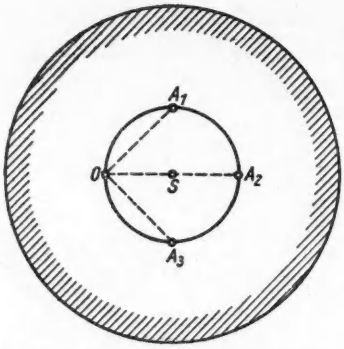

Fig. 3. **Circular path of bearing centre axis O of deflecting bar.**
S = centre of gravity, A_1, A_2, A_3 = points of travel of O on the circle.

In Fig. 4, point O again represents the bearing centre axis, S the centre of gravity, A the position of point O at the time t (corresponding to A_1 in Fig. 3). AS forms angle φ with the x-axis which has been drawn so that angle $\varphi = 0$ for time $t = 0$. Let the direction of rotation be such that φ increases with time t. Then

$$\varphi = \omega t;\ p = e \cos \omega t;\ q = e \sin \omega t.$$

If m is again taken as the mass of the eccentrically deflected part of the bar, then the basic dynamic equation, separated into x- and y- components, is

$$m \frac{d^2 x}{dt^2} = -c\,(x + p);\ m \frac{d^2 y}{dt^2} = -c(y + q)$$

where $x + p$ is the horizontal component of the restraining value AO, and $-c\,(x + p)$ that of the restraining force which is directed towards the origin O of the co-ordinate system.

The proportionality constant c of the restraining force can be calculated from the theory of elasticity if E, I, and eccentricity of deflection $e = OS = AS$ are known. Again disregarding the comparatively insignificant dead weight of the bar, we obtain the differential equation of the bar motion:

$$\frac{m}{c}\frac{d^2 x}{dt^2} + x + e \cos \omega t = 0;$$
$$\frac{m}{c}\frac{d^2 y}{dt^2} + y + e \sin \omega t = 0.$$

with the general solution:

$$\left.\begin{aligned} x &= A \sin \sqrt{\frac{c}{m}}\, t + B \cos \sqrt{\frac{c}{m}}\, t + e \frac{c/m}{\omega^2 - c/m} \cos \omega t \\ &= C \sin \sqrt{\frac{c}{m}}\, t + D \cos \sqrt{\frac{c}{m}}\, t + e \frac{c/m}{\omega^2 - c/m} \sin \omega t \end{aligned}\right\}$$

where A, B, C, D are integration constants determined by boundary conditions. The first two expressions on the right hand side of each of these solutions represent the natural harmonic vibration of the bar, which is only dependent on the initial conditions. The rotational speed does not enter into this part of the solution i.e., the vibration, once started by external causes,

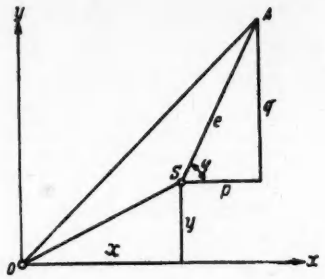

Fig. 4. **Co-ordinate system for the calculation of the bar motion.**
x, y = co-ordinate axes, e = eccentricity, p, q = normal projections of e, φ = angle between direction of e and x-axis, O = locus of bearing centre axis, A = locus of O at time t/e, S = centre of gravity.

would continue even if the bar were not to rotate. The centroid S describes an ellipse which, with suitable initial conditions, may transform into a circle. This natural vibration would not increase with rotational speed ω, but rather be damped by additional friction and air resistance. The last expression of each equation represents a forced vibration imposed by the rotational speed ω, which alone determines this part of the vibrations; initial conditions do not enter into it. If, after running for a short time, the natural vibration has been damped out, the remaining forced vibration

$$x_2 = r \cos \omega t;\ y_2 = r \sin \omega t;\ r = e \frac{c/m}{\omega^2 - c/m}$$

shows circular movement of the centroid S, on a radius r and with rotational speed ω. Immediately after a gear change the two parts of the vibration may be superimposed before the natural component has died away, and the centroid then moves on an epicycloid, i.e., on a circle the centre of which describes an ellipse. The amplitude of vibration depends on the radius r, which, at low speeds, is negative, with r slightly greater than e. At the critical speed

$$\omega_{cr} = \sqrt{c/m}$$

r becomes infinite, very large amplitudes must be expected, limited by damping resistances only. At over-critical speeds, r decreases again and, for very high speeds, is nearly zero. The centroid then describes the ellipse of the natural vibration, or after this has been damped out, coincides permanently with point O, the rotation being stable again.

Since speed changes are frequent with capstan and automatic lathes, dynamic conditions must be taken into account in the design of extension tubes. Immediately after speed changes, the bar material is suddenly accelerated, the epicycloidal movement of the centroid will lead to an increasing radius r, and the bar will hammer violently against the tube lining until, after reaching an over-critical speed and after damping of the natural vibration, the motion is stable again and the bar runs smoothly. Obviously, a plastic lining cannot withstand the shocks and wear for any appreciable time, and an elastic spring lining must be used. Practical experience corroborates the theoretical results, which can now be calculated at the design stage from the equations given. Other phenomena in rotating machine tool spindles can often be explained by the same process. Rough turning surfaces may be due to vibration phenomena at or near the critical speed. Lathe spindles should be calculated for critical speeds, and if long shafts are to be turned, the influence of the shaft material must be included in the calculation. Clean machining surfaces can only be obtained by turning at over-critical speeds.

New Materials, Processes and Equipment

NEW TILTING-HEAD HYDRAULIC PRESS

THESE new presses manufactured by Emmett Machine & Mfg. Inc., Akron, Ohio are the result of more than two years of intensive research and development work, and they feature positive safety devices as well as rapid operation and quality materials and workmanship.

MERIT press Model No. E-113 shown in the accompanying illustration is available in two sizes, having platens of either 14 × 14 inches or 24 × 24 inches. They have been designed for applications requiring high-speed operation, accuracy of mould register, convenience of loading, and ease of stripping moulded products from the press. Construction features include bronze bushing guides on lower platen ; annealed steel ram, cylinder, and head castings; and a completely self-contained packing cartridge which can be removed quickly and easily for replacement or maintenance.

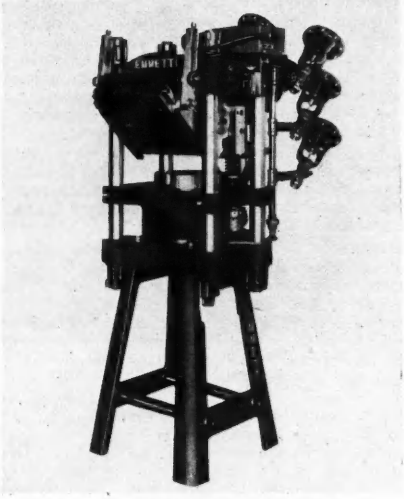

Operating speed of Model E-113 press is 3 seconds, including opening or closing of mould and tilting of head. Small press is stressed for a maximum pressure of 3000 psi and large press for a pressure of 2500 psi. Pull-back operation is accomplished by means of a telescopic ram located inside main ram. Normal stroke is 2½ or 6 inches in the 14 × 14 size, and 8 inches in the 24 × 24 size.

PANT-O-SCRIBER BLADE CHECKER

The Pant-O-Scriber Blade Checker, developed by the Engineers' Specialities Division of the Universal Engraving & Colorplate Co. Inc., Buffalo, N.Y., is an automatic machine which was built and then proven under actual production inspection line conditions. Its operation was clocked at 43 seconds for a 3 section blade, and blades were completely checked for contour, twist, thickness, width, etc., in less than one minute. A permanent inspection record of each blade is obtained at the same time as it is inspected.

The Pant-O-Scriber Blade Checker automatically traces the blade at the sections to be checked, and a co-ordinated rotating scriber automatically produces an exact scribing on a specially coated glass plate of each

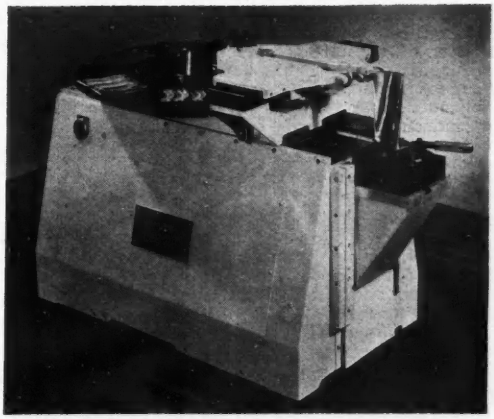

section as traced. The sections are scribed on the glass plate in relationship to the edge of the glass and to each other. The coating is a pleasant soft green colour.

A precision master inspection chart, actual size of the blade, is used together with the scribed plate for inspection purposes. The scribed plate and the inspection chart are placed face to face to a pre-determined registered position and the scribed blade profile and the master inspection chart are thus projected at any desired size on to a white opaque projection screen, using a standard make vertical lantern slide projector.

DIRECT READING DIAL

A simple, low-cost direct reading dial for use on all small and medium size lathes, milling machines and other machine tools is announced by Van Dyke Instruments, Glendale, California. The Revodex dial consists of two inter-geared dials, the first reading in thousandths of an inch is comparable to the standard dial on

most equipment. The second dial reads in tenths of an inch and indicates the actual number of revolutions of the first dial. In use, it relieves the operator from mentally adding the number of complete revolutions and eliminates the necessity of frequent micrometer checks. The Revodex speeds up dial setting, ensures accuracy, reduces work spoilage and provides a constant record of the total feed from zero position.

United Kingdom Engineering Exports to Canada

A REPORT of the United Kingdom Engineering Mission to Canada which spent seven weeks in Canada in the autumn of 1948 and, travelling 8,500 miles, visited the most important centres from coast to coast, has just been published by His Majesty's Stationery Office.

The Engineering Mission consisted of twelve members and was sponsored by the Board of Trade. The objects of the mission were to investigate market possibilities mainly for the heavier type of engineering equipment; to obtain first-hand information on any difficulties in regard to trade with Canada in the engineering industry, and to advise on the most suitable methods to adopt to secure a greater volume of exports from this country.

The leader of the Mission was Mr. E. H. Gilpin, Director of Baker Perkins Ltd., and Chairman of the British Food Machinery Manufacturers' Association.

The Members were:

Mr. N. Neville, Associate Organiser of the Mission, Director of the British Food Machinery Manufacturers' Association and also of the British Chemical Plant Manufacturers' Association.

Mr. E. Bruce Ball, Director of Glenfield and Kennedy Ltd.

Mr. A. W. Berry, Director of the British Engineers' Association.

Mr. W. R. Beswick, Director of the Power Gas Corporation and of Ashmore Benson Pease & Co., Ltd.

Mr. D. Maxwell Buist, Export Director of the British Electrical and Allied Manufacturers' Association, Inc.

Mr. F. C. Fitzpatrick, Amalgamated Engineering Union.

Mr. A. G. Grant, Director of Whessoe Ltd.

Mr. C. S. Robinson, Director of Thomas Robinson & Son, Ltd.

Mr. H. V. Yorke, Director of Bennett, Sons & Shears Ltd., and H. Pontifex & Sons Ltd.

Mr. C. Bennett, M.B.E., represented the Ministry of Supply, and Mr. P. S. Young, now United Trade Commissioner in Vancouver, accompanied the Mission throughout its tour in Canada. The Secretary of the Mission was Mrs. K. Gwynn-Jones.

The Report contains a Foreword by the President of the Board of Trade, Mr. Harold Wilson, who, after saying that "There is no more important market for U.K. goods to-day than Canada, and to increase our exports to her is a task of first-class national importance," refers to the unanimous opinion of the Mission that Canada offers a solid and expanding long-term market for our engineering goods.

The Report itself is an exceptionally valuable survey of the Canadian market. It gives not only concise and authentic information on the natural resources of the country, investment of external capital, population, production and transportation, sources of supply, etc., but contains a brief review of those Canadian industries that provide openings for the types of engineering equipment covered by the Mission. Public Utilities; Waterworks Plant; Road Construction; The Gas and Coking Industries; Bread and Flour Confectionery Industry; Biscuit, Chocolate and Sugar Confectionery Industry; Brewing and Bottling; Distilling; Mineral Water Machinery; Grain and Milling Machinery; Edible Oils and Fats Industry; Dairy Industry; Meat Packing Industry; Canning Machinery; Packaging, Wrapping and Labelling Machinery; The Iron and Steel Industry; Petroleum Industry; Chemical Industry, are chapters dealing with findings of the Mission in these particular industries Important sections of the industry, e.g., internal combustion engines, machine tools, mining and agricultural machinery, are not covered in the Report. In Appendix I, however, the number of establishments and 1946 value of products of the Canadian Industries based upon Iron and Steel and Non-Ferrous Metals is given.

The Dominion imports at least £100 m. of capital equipment annually.

The Report indicates ways and means for improving the lowly position we occupy in Canadian import returns to-day. It does not gloss over the difficulties in the way. The United States is now very strongly entrenched. In the opinion of the Mission, there is, however, a potential market, a promising, stable and increasing market for a wide variety of United Kingdom equipment. It will not be won without strenuous and sustained effort, and the Report indicates the various ways suited to the conditions of each case, by which the task may be approached.

What the Mission has done is to establish a new fund of goodwill in Canada, and an understanding, not perhaps, as yet, as complete as it should be, of the economic position.

It is difficult for a Canadian to understand why, when his country has made such immense sacrifices for us, we should be upsetting the whole economy of the Dominion by reducing our purchases of the products of its farms and forests. The Canadian sees, with puzzled amazement, our trade agreements with nations which spend their energy in reviling us. The Mission did everything in its power, not without a considerable measure of success, to explain why, in a world more and more tightly laced in the strait-jacket of bilateral trade, the trading accounts of two nations must come into some sort of balance. At every meeting with statesmen and industrialists, it was explained bluntly but politely that, as things are in the world, the only way we can pay Canada is by goods and services, and that the possibility of an increased volume of our purchases from her inexorably depends upon the increase of her purchases from us.

Even the limited acceptance of this explanation has established goodwill. Particularly in the Western and Maritime provinces, from which the bulk of supply to us has always come, the Canadian buyer, subject always to acceptable price, delivery and service, is more than ready to buy British. It is now up to the British manufacturer to deliver the goods.

This whole task is much more than an ordinary commercial undertaking. It is no exaggeration to say that the limitation of purchase from Canada, if long continued, might eventually threaten the whole structure of the Commonwealth. It becomes, therefore, a national duty, which the engineering industry must accept, to increase its service in Canada to the greatest possible extent. That stark but exhilarating prospect is at the very centre of the Mission's message.

It is admittedly a great venture, for both Britain and Canada. In recent years we have both followed the lines of least resistance. British order books have been filled from our easy and traditional markets, Canada has supplied her needs across the unguarded frontier of the 49th parallel. We have both to change our ways.

It must not be expected that the venture will show immediate and spectacular results. "Sweat and tears," although, fortunately, not "blood" must be endured. The heights will not be "attained by sudden flight." Operation Canada is no hit-and-run raid. It is to be a long-term enterprise, backed by all the resources of Government and industry. Meetings will be held in the principal centres of the industry, which members of the Mission will address. Each member is ready to give personal advice to individual firms and trade associations. They feel that their tour of Canada was only the beginning of their task. As the leader of the Mission often said to Canadians, "We came out as a Mission to Canada. We go back as a Mission to Britain."

Continued on page 70

CLASSIFIED ABSTRACTS

Numerous important abstracts which, for lack of space, cannot be published in our main editorial columns, are regularly included in condensed form in this section. Subscribers may obtain photostat copies of all original articles at cost.

ABRASIVES

Theory and Practice of the Crush Dressing Operation on Grinding Wheels

By E. C. HELFRICH. (From *ASME Transactions*, Vol. 70, No. 8, November, 1948, pp. 885-891, 7 illustrations.)

THIS paper presents a qualitative analysis of the crush-dressing process based upon experimental evidence. The theory developed therein accounts for the forces involved, power requirements, rate of wheel removal, the effect of wheel and crusher diameters, and surface speed in the crushing process. The equations and data presented will enable the designer to engineer crush-dressing applications more intelligently, and will contribute to a clearer understanding of the process by all who may be interested in applying it. The advantages and disadvantages of crush-dressing versus diamond truing are discussed with reference to the physical properties of crystals.

GAS TURBINES

Thermodynamic Properties of Gas Mixtures Encountered in Gas Turbine and Jet Propulsion Processes

By J. KAYE. (From *Journal of Applied Mechanics, Transactions ASME*, Vol. 15, No. 4, December, 1948, pp. 349-361, 10 tables, 1 illustration.)

THE presentation of data for gas mixtures on a molal basis reduces greatly the number of gas tables required for calculations of processes in a wide variety of mixtures. This simplification of the tabular data is illustrated in detail by consideration of several gas mixtures and of the processes encountered in the design of gas turbines. Three tables of products of combustion of a hydrocarbon fuel with air are sufficient to permit calculations of all processes of interest, with an average error of about 0·1 per cent over a large range of hydrogen-carbon ratios of the fuel and over the range of fuel-air ratios for lean mixtures. Furthermore, these three tables may be used with the same error for calculations involving mixtures of air and octane vapour as well as for mixtures of air and water vapour.

IRON AND STEEL

Identification of Carbon Steels by the Spark Test

By W. JÄNICHE and K. H. SAUL. (From *Stahl und Eisen, Germany*, Vol. 68, No. 17/18, August 12, 1948, pp. 301-303, 9 illustrations.)

THE grinding sparks of carbon steels are a well-known, quick and cheap medium for identifying steels of different carbon content, provided the latter need not be known within very accurate limits. Soft iron emits the familiar spear-like tracer sparks, whereas with increasing carbon content, explosive star-like carbon sparks appear and increase in frequency and size. The spark emission cannot be photographed with sufficient clarity, but characteristic drawings can be made and testers can be given a set of steels of known composition for comparative purposes. An experienced tester can distinguish steps of 0·05 per cent carbon in steels containing up to 0·35 per cent of carbon. In steels from 0·35 to 0·60 per cent, steps of 0·10 per cent carbon can be distinguished. Silicon additions (1·3 per cent) give a characteristic yellow spark colour; manganese steels (1·3 per cent Mn) can be identified by their extremely bright short spikes. With steels containing above 0·60 per cent of carbon, silicon and manganese additions can still be identified, but co-ordination within a definite range of carbon percentages is not possible. For the tests, grinding disks of medium grain and of a fairly high degree of hardness, about $2\frac{1}{2}$ inches in diameter and $\frac{1}{4}$ inch in width, are recommended. Very large disks produce too many sparks and blur the picture. Systematic training of testers showed that 20 hours' training (2 hours per day), periodically repeated, is quite sufficient to reduce the number of errors in judgment to a minimum, i.e., four out of a hundred tests for good testers.

METALLURGICAL ENGINEERING

Coating Steel with Nickel by Immersion in Nickel Chloride Solutions

By W. A. WESLEY and H. R. COPSON. (From *Journal of the Electrochemical Society, U.S.A.*, Vol. 94, No. 1, July, 1948, pp. 20-31, 4 illustrations.)

A SIMPLE method for depositing controlled amounts of nickel on steel by chemical displacement from a hot nickel chloride, boric acid solution is described. Deposits up to 30 millionths of an inch (0·75 micron) in thickness can be readily produced in this way. Suitable heat treatment of these deposits renders them compact and adherent and at the same time causes diffusion of the nickel and iron. Although steel coated in this way rusts readily, its surface is altered sufficiently to suggest that it will serve as a better basis for other coatings, such as organic finishes, conversion coatings, ceramic enamels and perhaps for other metallic coatings. The optimum degree of alloying of the nickel and iron varies with the intended use of the product.

OPTICS

High-Resolution Camera for Structural Analysis by Monochromatic X-Rays

By E. E. VAINSHTEIN and K. I. NARBUTT. (From *Zavodskaya Laboratoria, Russia*, No. 5, 1947, pp. 588-589, 1 illustration.)

STRICTLY monochromatic X-ray analysis is important for many problems connected with the theory of the solid and liquid state, and of vitreous substances, but existing methods have not succeeded in combining strict monochromatisation with high resolution. The authors have shown that the problem may be solved by combining Guinier's suggestion of using a curved crystal as monochromator with the axial method of focussing first used by Hulubei and Gouy. The authors' spectrograph has recently been simplified so as to serve as a powerful monochromator.

An analytical X-ray tube with an annular focus serves as the source of X-rays and this ensures a high output by permitting a close approach of the source to the crystal. The latter is given cylindrical form (e.g. a mica foil wrapped around a circular sharp-edged disc with about 0·1 mm clearance), and represents the

TESTAL

Aluminium Alloys

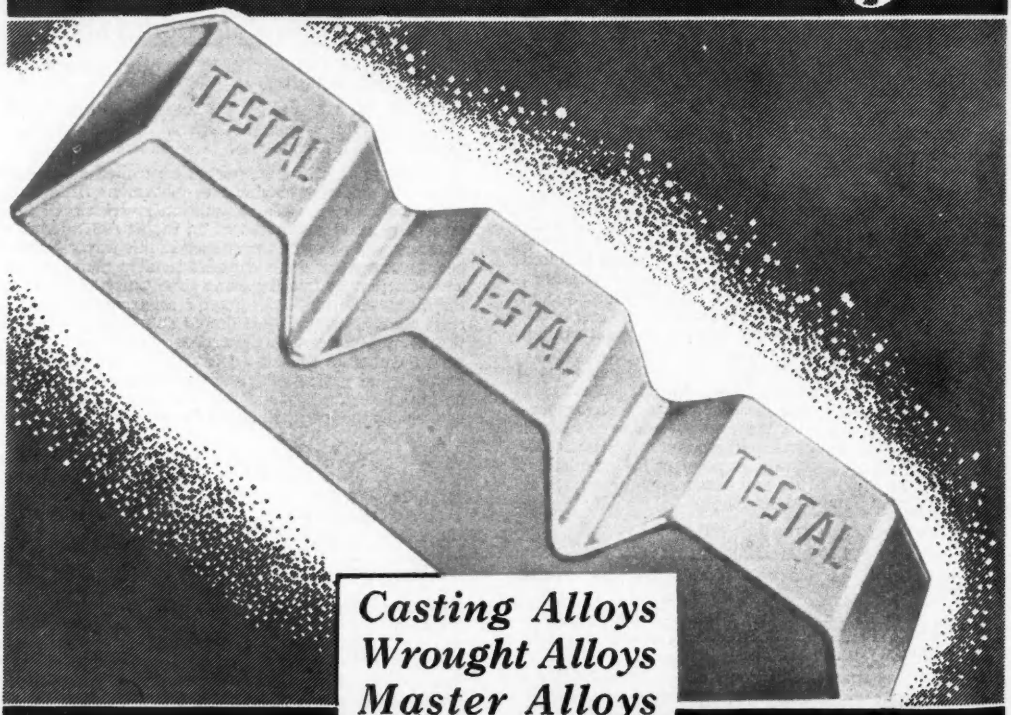

Casting Alloys
Wrought Alloys
Master Alloys

B·K·L·ALLOYS LIMITED

FACTORY CENTRE · KINGS NORTON · BIRMINGHAM 30

TEL·KIN 1162/5

monochromator based on Bragg's principle of monochromatisation by preliminary reflection on a flat crystal. Whether or not an annular focus is suitable depends on the distance of the imaginary focus O_1 from the crystal. For a given radius R of the cylindrical crystal, this distance varies with Bragg's angle α dedetermining the reflection of radiation of a given wavelength, according to the relation $l = R \cot \alpha$, where l is the distance mentioned.

For small distances l, the annular focal plate can be replaced with advantage by a punctiform plate, placed at the imaginary focus O_1. The cone of rays emitted by the tube strikes the crystal at the Bragg angle α, and, after reflection, represents a cone of monochromatic rays. Adjustment to a given wavelength is obtained by displacing the focus relative to the crystal and thereby changing the Bragg angle.

A flat polycrystalline object, or a container with a liquid specimen placed in the path of the monochromatic rays, gives rise to a series of Debye cones, the apexes of which lie at the circular intersection of the cone of rays with the object plane. These Debye cones are due to the reflections in the various crystallographic planes, and the cones of any individual family will have a common point F_i on the axis. The envelope of each family (itself conical) is then the locus of increased intensity of the radiation, the F_i's being foci of interference of the rays, i.e., maxima of intensity. A film arranged along the axis of the apparatus will show a series of cruciform reflections corresponding to the intersection of the envelope of the Debye cones with the plane of the film. The annular focal plate is thus more suitable for analyzing liquids and vitreous substances where the main interest lies in the lines close to the straight pencil of rays, while the punctiform focus will be preferred for work at large Bragg angles. The formula relating to the spread of the diagram in terms of the distance l_i of the individual interference maximum from O, the point of intersection of the plane of the film with the apex of the cone of the primary monochromatic rays permits of determining the corresponding Bragg angles. It is

$$l_i = a \left[1 - \frac{\tan \alpha}{\tan (2\,\vartheta_i + \alpha)} \right]$$

where a is a geometrical constant of the camera, α the Bragg angle used in the monochromator, and ϑ_i the Bragg angle corresponding to the given interference maximum of the radiogram.

POWDER METALLURGY

Production of Electrolytic Iron Powder

By G. WRANGLÉN. (From *Jernkonterets Annaler, Sweden,* Vol. 132, No. 12, December, 1948, pp. 501-516, 10 illustrations.)

ELECTROLYTIC metal powders can be produced either by direct deposition at the cathode or by grinding of a coherent deposit. In the case of iron, the latter method is the simplest and cheapest, and although there are many patents dealing with the direct deposition of iron powder, there is no evidence that this method is in commercial use. In the investigation presented in this paper, both methods have been tried, and detailed information is given for the conditions of electrolysis in both cases.

For the direct deposition of iron powder the following conditions are recommended: 15 gram/litre Fe as $FeCl_2$, 100 g/l NH_4Cl, 50° C, pH 7 (2-3 g/l of the iron as hydroxide), 100 amp./sq. ft. The current efficiency is 95 per cent. With an electrode distance of 1·2 in. the cell voltage is 2 volts, which means a power consumption of about 1 kWh per lb of iron. The formation of powder on the cathode in this case is due to the precipitate of hydroxide in the cathode film. For the production of a coherent but brittle deposit, which can be easily comminuted to a fine powder, the following conditions are recommended: 60 g/l Fe as $FeCl_2$, 50 g/l NH_4Cl, 60° C, pH 5-6, 30 amp./sq. ft. With an electrode distance of 1·6 in. the voltage is 0·9 volts and the power consumption is about 0·5 kWh per lb of iron. In both cases, soluble anodes of mild steel have been used.

The influence of the structure of the deposited iron on the shape of the powder particles is discussed. The powdery deposits obtained on the cathode consist of tree-like formations which, after breaking up, will yield a powder of substantially equi-axial particles. The fibrous structure of the normal deposit gives long needle-like particles after grinding, which are undesirable from a powder-metallurgical point of view. Three methods (a, b, c) are proposed for modifying the fibrous structure, so that nearly equi-axial particles will be obtained after grinding. This may be done by cutting off the long acicular crystals with intermediate layers of oxide (a) or another metal (b) or by dispersing in the electrolyte an electrically conductive substance (c), such as a finely divided metal or carbon powder, which will change the structure from a fibrous one to an irregular mosaic structure.

In the discussion of the industrial application of the results obtained, special attention is given to the anode material and the anode process. Although scrap iron is intended as raw material, the use of insoluble anodes is considered for various reasons as less promising than a process based on the use of scrap iron as soluble anodes, which is described in some detail.

REFRIGERATING ENGINEERING

Ice-Making by the Extrusion Process

By J. R. WATT. (From *Mechanical Engineering, U.S.A.*, Vol. 71, No. 1, January, 1949, pp. 17-20, 4 illustrations.)

THE author's experiments at the University of Texas since 1943 have resulted in the development of a continuous process for generating ice cakes where no labour is involved and the use of brine or ice cans is unnecessary. Direct-expansion freezing cylinders extrude hard white ice in continuous columns suitable for automatic severing into cakes. A water film approximately 6¼ in. thick is developed in the machine and freezes in 10 to 15 seconds on a previously prepared core of ice. For each stroke of the machine a successive new layer of ice, the "incremental film," freezes integrally to the one before. Each cycle, therefore, adds new ice below and around the core, forming a column which is extruded upwards step by step from the cylinder. About 4 to 5 cycles per minute gave optimum output.

The advantages of this method in comparison with other continuous ice-generating systems are discussed and the author comes to the following conclusions:—

Tests so far conducted suggest that the following economical advantages are probable:

(1) Building space requirements will be reduced by about 80 per cent.
(2) The equipment will be cheaper than a brine tank and cans.
(3) There is one auxiliary, not several.
(4) There is no foreseen corrosion problem.
(5) Labour costs will be reduced.
(6) Existing compressors, etc., may be used.
(7) Installation costs will be low.
(8) Refrigeration losses, radiation, etc., will be reduced.

As far as is known, this is the only existing process for the automatic production of ice cakes. It should be applicable wherever white ice is acceptable.

. . . and **SALTER** *for dependability in* *springs*

GEO. SALTER & CO. LTD., WEST BROMWICH

NEWS OF THE MONTH

PERSONAL

Mr. C. S. Anderson, of Anderson, Green & Co., 7, Bishopsgate, London, E.C.2, has been elected President of the Chamber of Shipping in the United Kingdom. **Sir Guy Ropner** has been elected vice-president.

Sir Edward Appleton, M.A., D.Sc., F.R.S., Secretary of the Department of Scientific and Industrial Research, is shortly taking up the position of Principal of the University of Edinburgh.

Mr. John Benstead, C.B.E., M.Inst.T., has been appointed to be the first deputy chairman of the British Transport Commission.

Mr. H. H. Bruce has been elected President of the Institution of Heating and Ventilating Engineers.

Mr. James Calderwood, M.Sc., M.I.N.A., M.I.Mar.E., A.F.R.Ae.S., has been appointed technical director of Associated British Oil Engines Ltd. Mr. Calderwood will be in charge of design and development at each of the five factories of the Company where the Mirrlees, McLaren, Petter and Petter-Fielding diesel engines are at present being built.

Mr. Arthur Chamberlain, managing director of the Hercules Cycle and Motor Co., Ltd., has been elected a director of Tube Investments Ltd.

Sir Charles Darwin, M.A., D.Sc., F.R.S., who has been Director of the National Physical Laboratory since 1938, is retiring on the 31st March.

Mr. T. H. Eccles has been appointed manager of the London office of Musgrave & Co., Ltd., 1a, Newman Street, London, W.1.

Mr. H. B. Everard, D.S.O., B.A. (Cantab.), A.M.I.C.E., has been appointed chief officer engineering (maintenance) of the Railway Executive.

Dr. F. A. Fox, deputy director of the British Welding Research Association has been appointed deputy technical manager of H. J. Enthoven & Sons, Ltd., 15, Lime Street, London, E.C.3.

Mr. S. W. Fryer, Northern Area manager of Wellworthy Piston Rings Ltd., Lymington, has assumed control of all the firm's service branches. He has been succeeded by **Mr. J. A. Dobbie** as Northern Area manager at 211, Bothwell Street, Glasgow.

Professor W. R. Hawthorne, B.A. (Cantab.), Sc.D.(M.I.T.), has been appointed Director of the Whitworth Laboratories in the University of Manchester.

Mr. H. W. G. Hignett, B.Sc., superintendent of the research and development department laboratory of the Mond Nickel Co., Ltd., Birmingham, has been elected to the Council of the Institute of Metals.

Mr. O. W. Humphreys, B.Sc., F.Inst.P., A.M.I.E.E., has been appointed manager of the Research Laboratories of The General Electric Co., Ltd., at Wembley, Middlesex. He will be advised by a small scientific panel of his colleagues, of which **Dr. B. P. Dudding** is vice-chairman.

Mr. Michael C. Lloyd has been appointed director and general manager of the Weldless Steel Tube Co., Ltd., and Tube Rolling Mills Ltd., Wednesfield, Staffs.

Mr. W. K. B. Marshall, B.Eng.(Liv.), A.I.M., has been appointed assistant director of research of the British Welding Research Association, 29 Park Crescent, London, W.1.

Mr. Peter G. Masefield, M.A., F.R.Ae.S., has been appointed assistant to the chairman and general manager of British European Airways Corporation.

Mr. W. R. McGraw, A.F.R.Ae.S., has been appointed director of aircraft production, Ministry of Supply.

Mr. J. Morris, works manager of the Crewe works of Rolls-Royce Ltd., has been appointed director of technical research and development with Sentinel (Shrewsbury) Ltd., Shrewsbury.

Mr. Arthur Offen has established a tool design consultant's office at 47, West Street, Dorking, Surrey.

Mr. C. W. Pass, M.B.E., B.Sc., A.M.I.E.E., has been appointed manager for Crompton Parkinson Ltd., in South America. His address is c/o Crossley Bros. Ltd., Cassilla de Correo 472, Buenos Aires.

Mr. Henry Spurrier has been appointed managing director of Leyland Motors Ltd., Leyland, Lancs., and retains his position of general manager of the Company. **Mr. C. B. Nixon** is continuing as chairman and governing director.

Mr. R. C. Stanley has relinquished his position as President of the International Nickel Company of Canada, Ltd., but continues as chairman of the board. **Dr. J. F. Thompson** has been elected President, and **Dr. P. D. Merica** has been made executive vice-president. **Sir William Griffiths** continues as vice-president in charge of operations and activities in Europe and other parts of the world outside the American continent.

Sir Robert Watson-Watt, C.B., F.Inst.P., M.I.E.E., F.R.Ae.S., F.R.S., has been elected President of the Royal Meteorological Society, 49, Cromwell Road, London, S.W.7.

BUSINESS NOTES

The India Supply Commission, a department of the High Commissioner for India in the United Kingdom, have moved into new premises at 55, Jermyn Street, London, S.W.1. Tel. : REGent 8250.

The British Empire Chamber of Commerce in the U.S.A. has changed its name to The British Commonwealth Chamber of Commerce in the U.S.A., Inc., 55, Broadway, New York 6, N.Y., U.S.A.

Nelson Stud Welding Service. Crompton Parkinson Limited, Crompton House, Aldwych, London, W.C.2, have taken over the Nelson Stud Welding Service.

British Celanese (Overseas) Ltd. The Directors of British Celanese Ltd. have decided, in view of the increasing importance of the Company's export trade, to form a wholly-owned Subsidiary, British Celanese (Overseas) Ltd. with £100,000 capital.

Mr. G. H. Spilman (Chairman), Mr. R. T. Archer, Mr. W. F. Archer, Mr. A. T. Brenchley, Mr. C. H. Colton, Mr. W. A. Dickie, Mr. G. Donnelly, Mr. T. P. Jennison and Mr. M. Spilman will be directors of the new Company which will commence trading on the 1st April, 1949.

Flexibox Limited, mechanical engineers and manufacturers of "Flexibox" mechanical seals for rotary pumps and compressors, have recently moved to their new works and offices in Nash Road, Trafford Park, Manchester, 17.

The Hopkinson Electric Co., Ltd., of Birchgrove, Cardiff, have opened new branch offices at 41 John Dalton Street, Manchester (Tel. : Blackfriars 4638), and at 11 Park Place, Leeds (Tel. : 28712). Mr. T. C. Beaumont, A.M.I.E.E. has been appointed in charge of the Manchester office, and Mr. J. Grant, of the Leeds office. The following new appointments have also been made :— Mr. D. F. Bentley, assistant works manager ; Mr. P. A. Adams, London sales engineer ; Mr. D. S. Nelson, area sales engineer (S.E. London and S.E. Counties) ; Mr. S. R. Bond, area sales engineer (Nottingham, Derby, Leicester, Lincoln, Rutland) ; Mr. L. Byrnes, A.M.I.E.E., area sales engineer (Cumberland, Northumberland, Westmorland, Durham) ; Mr. T. P. C. Hornsby, area sales engineer (S. Wales) ; and Mr. R. I. Brydon, asst. sales engineer (Manchester).

Thos. W. Ward Ltd., Albion Works, Sheffield, have taken over world sales distribution for Eldair press brakes and for precision gauges manufactured by K. Emsley Ltd., Bradford.

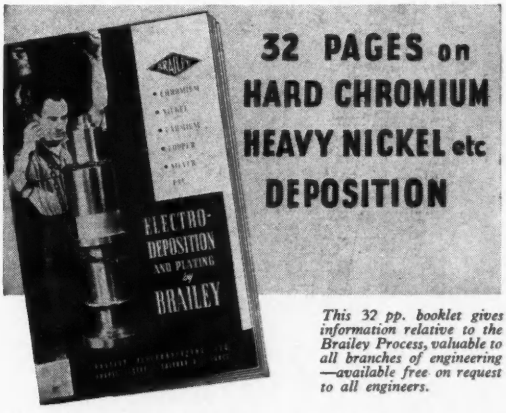

32 PAGES on HARD CHROMIUM HEAVY NICKEL etc DEPOSITION

This 32 pp. booklet gives information relative to the Brailey Process, valuable to all branches of engineering —available free on request to all engineers.

● CHROMIUM ● NICKEL
● CADMIUM ● COPPER
● SILVER ETC.

BRAILEY (Regd)

The Brailey process of building-up worn or undersized parts or for protecting parts against wear or corrosion gives a molecular interlocking between metal and deposit, which can be of substantial thickness.

BRAILEY ELECTROPLATERS LTD.
CHAPEL ST · SALFORD 3 · LANCS.

B34

Gandy Ltd., Wallasey, Cheshire, have removed their Leeds office to new premises at 9, Somers Street, Leeds 9.

Hills Patent Glazing Co., Ltd., has changed the name of the company to Hills (West Bromwich) Ltd. Under this name are incorporated Universal Steel Door & Engineering Co., Ltd.; Accordo Blinds Ltd.; Hilcon Ltd.; Chain Developments Ltd.; and Wottons (Croydon) Ltd.

E.M.I. Technical Papers. Reprints of Technical Papers read by members of the Staff of Electric & Musical Industries Ltd., before learned Societies are now available at 2s. 6d. per copy. These papers are printed on art paper with a semi-stiff cover, and are well illustrated. The titles at present available are :—

Commercial Disc Recording and Processing	B. E. G. Mittell.
The Development of Sound Recording and Reproduction	Sir Ernest Fisk.
Sound Recording and Reproduction	G. F. Dutton.
High Quality Disc Recording	W. S. Barrell.

Others will be produced in due course.

Applications for copies of the above should be addressed to Advertising Division, E.M.I. Sales & Service Ltd., Hayes, Middlesex.

The Nickel Bulletin. The December issue of The Nickel Bulletin completes Volume 21, 1948. This issue contains the complete index of subject matter for the year, published under the headings of Subject, Author and Patents. Abstracts cover applications of nickel-containing materials in reference to chemical and railway engineering, the electrical, petroleum and motor industries, paper mills, sewage plants, among other subjects.

Copies of The Nickel Bulletin are obtainable, free of charge, on appplication to The Mond Nickel Co., Ltd., Sunderland House, Curzon Street, London, W.1.

United Kingdom Engineering Exports to Canada.

(Continued from page 66.)

A synopsis of the Mission's recommendations appear below. The report will repay study, both by the engineering firms to whom it is primarily addressed and also by those engaged in many other industries, for the need to increase exports to Canada exists in all fields of commercial endeavour. It contains detailed advice on many industrial market features, two informative maps, statistical appendices, and a note on other useful sources of information.

CONCLUSIONS AND RECOMMENDATIONS

In a section on Conclusions and Recommendations, the Report says there is an important, stable and growing market in Canada. It is, however, a difficult market. The buying centres are far apart. The Canadian engineering industry is strong and versatile. The United States is a formidable competitor with whom it will need skill and energy to compete. The work of the Mission must be followed up by more detailed investigation and then by action. The national need demands that the United Kingdom manufacturer makes every possible effort to increase the export of engineering equipment to Canada.

Finally, the Mission makes the following recommendations :—

Delivery promises for Canadian orders in hand should be kept and, if necessary, improved.

Immediate and special attention should be given to enquiries received from Canada.

On publicity it is emphasized that :

(a) Appropriate literature should be circulated to prospective customers in Canada, and

(b) That publishers of United Kingdom technical and trade press should take steps to expand their circulation in Canada.

Young Canadian engineers should be invited to put in a term at United Kingdom engineering works as a form of post-graduate training.

United Kingdom manufacturers of engineering equipment should arrange to visit Canada in the spring of 1949 to explore the market for their products and arrange for effective representation.

Every section of the engineering industry should take early steps to study the Canadian market for its products.

And, finally, appropriate sections of the United Kingdom engineering industry should maintain specialist representatives in Canada.

EXECUTIVES, technical training officers, and works librarians who are constantly seeking the newest technical publications will find a quick and competent service at any branch of W. H. Smith & Son.
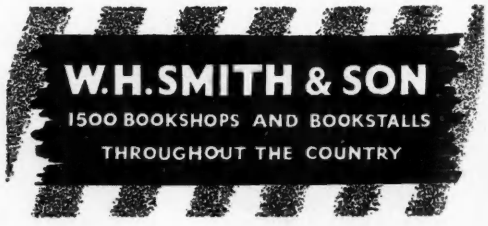
Each is in daily contact with Head Office in London and your orders, either for single copies or complete works libraries will be fulfilled within the shortest possible time.